INTERVAL METHODS FOR RIGOROUS INVESTIGATIONS OF PERIODIC ORBITS

ZBIGNIEW GALIAS
Institute for Nonlinear Science, University of California, San Diego
9500 Gilman Dr., San Diego, CA 92093-0402, USA
e-mail: galias@ucsd.edu
permanent address
Dept. of Electrical Engineering, University of Mining and Metallurgy
al. Mickiewicza 30, 30–059 Kraków, Poland

Abstract

In this paper, we investigate the possibility of using interval arithmetic for rigorous investigations of periodic orbits in discrete–time dynamical systems with special emphasis on chaotic systems. We show that methods based on interval arithmetic when implemented properly are capable of finding all period-n cycles for considerable large n. We compare several interval methods for finding periodic orbits. We consider the interval Newton method and methods based on the Krawczyk operator and Hansen–Sengupta operator. We also test the global versions of these three methods. We propose algorithms for computation of the invariant part and nonwandering part of a given set and for computation of the basin of attraction of stable periodic orbits, which allow reducing greatly the search space for periodic orbits.

As examples we consider two–dimensional chaotic discrete–time dynamical systems, defined by the Hénon map and the Ikeda map, with the "standard" parameter values for which the chaotic behavior is observed. For both maps using the algorithms presented in this paper, we find very good approximation of the invariant part and the nonwandering part of the region enclosing the chaotic attractor observed numerically. For the Hénon map we find all cycles with period $n \leq 30$ belonging to the trapping region. For the Ikeda map we find the basin of attraction of the stable fixed point and all periodic orbits with period $n \leq 15$. For both systems using the number of short cycles, we estimate its topological entropy.

1 Introduction

Finding periodic orbits of nonlinear systems is an important problem encountered frequently in a variety of fields. In particular the problem of existence of periodic orbits is crucial for analysis of chaotic systems, which under certain assumptions are characterized by the existence of infinitely many unstable periodic orbits embedded within the chaotic attractor. The structure of the strange attractor is built on an infinite set of unstable periodic orbits. Periodic orbits are ordered hierarchically, longer orbits give better approximations to the chaotic attractor. The problem of existence of periodic orbits is also of great importance in many applications. In the area of chaotic systems one could mention controlling chaos by stabilization of one of infinitely many periodic orbits embedded in a chaotic attractor [Ott et al., 1990] or using periodic orbits as a communication alphabet in a chaos communication scheme [Hayes & Grebogi, 1995].

Usually periodic orbits are found in numerical studies but there is no guarantee that there exists a true periodic trajectory that stays near a computer–generated one. This problem is especially important for chaotic systems, as due to inevitable round–off errors and sensitive dependence on initial conditions usually after certain number of iterations (100 or so) the computer–generated trajectory becomes uncorrelated with the true trajectory. A very important question is whether there really exists a true periodic trajectory in the neighborhood of the computer–generated one.

A method to find periodic solutions form a time series was developed in [Lathrop & Kostelich, 1989]. In this method one searches for parts of a trajectory which are almost periodic (the trajectory returns close to the initial point). The method is based on the assumption that in the neighborhood of such a fragment there exists a real periodic orbit. However, one never knows if a real trajectory actually exists. For example, in a quasiperiodic motion defined on the two-dimensional torus the method of close returns would find many periodic orbits but we know that there exists no periodic orbit for this system.

The basic numerical method for detection of period–n orbit of a map f is based on the Newton method for searching for zeros applied to the function $g(x) = x - f^n(x)$. The process of finding periodic orbit begins with the choice of initial point followed be computation of successive corrections. The method has very good convergence properties (the convergence is quadratic), assuming that the initial point is sufficiently close to the periodic orbit. We have however no rigorous proof that the periodic orbit exists. In order to find all periodic orbits one can check many initial conditions for example using a uniform grid. Again it is not sure that all periodic orbits are found.

There are several methods, which can be used for proving rigorously the existence of periodic orbits. Many of them are a simple conclusion of the Brouwer's fixed point theorem, which states that if a convex compact set $X \subset \mathbb{R}^n$ is mapped by a continuous map f into itself then f has a fixed point in X (i.e., there exist $x \in X$ such that $f(x) = x$). Using this theorem one can easily prove the existence of a stable periodic orbit. If the orbit is asymptotically stable one can find a neighborhood U such that $f^n(U) \subset U$, proving that there exists period–n point of f in U. Similarly, if the map is invertible one can prove the existence of a periodic orbit unstable in all directions (it becomes stable when the direction of time is changed). Unfortunately, this method cannot be used directly for proving the existence of saddle type orbits.

Another class of methods is based on the fixed point index properties. In one of the methods one has to prove the topological conjugacy of the map in the neighborhood of the fixed point with a linear map possessing a saddle–type fixed point [Miranda, 1940, Galias et al., 1994]. The second method involves computation of an integral of a certain function over a circle surrounding a fixed point of the map. If this integral is non-zero then the existence of the fixed point is ensured [Krasnosielskij, 1963]. This last method can be used when the map is two–dimensional. Both methods allow proving the existence of all types of periodic orbits (also of the saddle–type). Their main drawback is non-efficiency — one has to perform a lot of calculation in order to prove the assumptions of the existence theorem and control the computational error (in case of a computer assisted proof).

The recent development of new interval methods for proving the existence and uniqueness of zeros of nonlinear functions have opened the possibility of rigorous investigations of chaotic systems in terms of unstable periodic orbits. We compare several interval methods, which can be used for finding all low–period cycles of a nonlinear map. The main criterion is the computation time needed to find all period–n orbits in the considered region. In Sec. 2 we present a short introduction to interval arithmetic. We briefly recall the definitions of the interval operators and show how to use these operators and bisection technique to find all periodic orbits for given period. We test methods based on the interval Newton operator, the Krawczyk operator and the Hansen–Sengupta operator. We also consider the so–called global versions of these methods, where the problem of existence of periodic orbits is translated to the problem of existence of zeros of a higher–dimensional map. We introduce a modification where the dimension of the search space for the global version is reduced to the dimension of the original dynamical system. We also describe improvements useful especially if the map is invertible and if we know a trapping region of the system.

In Sec. 3 we present algorithms for computation of invariant and nonwandering part of a given set and an algorithm for computation of the basin of attraction of stable periodic orbits, which may significantly reduce the search space for periodic orbits.

In Secs. 4 and 5 we use the algorithms presented in this paper to study the existence of periodic orbits for the Hénon map and the Ikeda map. For both systems, we find very tight enclosures of the invariant and nonwandering parts of the trapping region in which chaotic behavior is observed. We also find all low period cycles and estimate the topological entropy of both maps.

2 Inclusion Methods for Proving the Existence of Periodic Orbits

In this section we present different interval methods for finding periodic solutions of discrete–time dynamical systems. Let us start by a short description of interval arithmetic — a basic computational tool used in this study.

2.1 Interval arithmetic

Interval arithmetic is a growing branch of applied mathematics developed to satisfy the demands on numerical computations to obtain rigorous results. Computations in properly rounded interval arithmetic produce results, which contain both machine arithmetic results and also true (infinite arithmetic precision) results.

Here we present a very short introduction to the interval arithmetic (for the thorough presentation see [Moore, 1979] or [Alefeld & Herzberger, 1983]). In this paper, we use boldface letters to denote intervals, interval vectors, and interval matrices and usual math italic lowercase letters to denote "real" quantities. By an *interval* we mean a closed bounded set of real numbers

$$\mathbf{x} = [a, b] = \{x \colon a \leq x \leq b\}.$$

We can also regard interval as a number represented by the ordered pair of its endpoints a and b. By an *n–dimensional interval vector* we mean an ordered n–tuple of intervals $\mathbf{v} = (\mathbf{x}_1, \mathbf{x}_2, \ldots, \mathbf{x}_n)$.

On the set of intervals we define basic arithmetic operations.

$$\mathbf{x}_1 \diamond \mathbf{x}_2 = \{x = x_1 \diamond x_2 \colon x_1 \in \mathbf{x}_1, x_2 \in \mathbf{x}_2\}. \tag{1}$$

where $\diamond$ is any of the following operators: $+$, $-$, $\cdot$, $/$. All operations but division are defined for arbitrary intervals. For the division we assume that the interval $\mathbf{x}_2$ does not contain the number 0. Since a real number a can be treated as a degenerate interval $a = [a, a]$ the interval arithmetic contains usual "real" arithmetic.

The result interval can be always computed in terms of the endpoints. For example, the rule for interval addition is following:

$$[a, b] + [c, d] = [a + c, b + d].$$

In practice we cannot carry out "real" or interval operations exactly. We are confined to approximate arithmetic of limited precision. It is possible to implemented interval arithmetic on a computer to carry out the operations of interval arithmetic with appropriate rounding, when necessary, of left and right computed endpoints, in such a way that the machine computed interval result always contain the exact interval result. In the "best" rounded interval arithmetic the machine computed right endpoint is the smallest machine number not less than the correct right endpoint and similarly the machine computed left endpoint is the largest machine number not greater than the correct left endpoint. There are many programming packages, which can be used for interval computations. They are available as libraries for C, C++, Fortran, and as a Matlab toolbox.

Some interval algorithms are extensions of corresponding real algorithms. Some of them however are essentially different. The difference results from a dual nature of an interval. As an interval is not only a number represented by its endpoints but also a set of real numbers, we can compute the intersection of two or more intervals or check the inclusion of one interval in another. Self–validating methods called also inclusion methods for proving the existence of zeros belong to this class.

Let us now introduce interval Newton operator, Krawczyk operator and Hansen–Sengupta operator [Alefeld, 1994, Neumaier, 1990], which provide simple computational tests for uniqueness, existence, and nonexistence of a zero of a function within a given interval vector.

2.2 Interval Newton operator

Let us consider a function $\mathbb{R}^m \ni x \mapsto f(x) \in \mathbb{R}^m$. In order to investigate the existence of zeros of f in an m-dimensional interval vector $\mathbf{x}$ one evaluates the *interval Newton operator*

$$\mathbf{N}(\mathbf{x}) = x_0 - (f'(\mathbf{x}))^{-1} f(x_0), \tag{2}$$

where $f'(\mathbf{x})$ is the interval matrix containing all Jacobian matrices of the form $f'(x)$ for $x \in \mathbf{x}$ and x_0 is an arbitrary point belonging to the interval vector $\mathbf{x}$. One usually chooses x_0 to be the center of $\mathbf{x}$.

One should notice that it is not necessary to compute the inverse of $f'(\mathbf{x})$ in order to evaluate $\mathbf{N}(\mathbf{x})$. For computation or the expression $(f'(\mathbf{x}))^{-1} f(x_0)$ one can use for example the Gaussian algorithm.

The following theorem [Neumaier, 1990, Alefeld, 1994] can be used to prove the existence and uniqueness of zeros of f.

Theorem 1. *If* $\mathbf{N}(\mathbf{x}) \subset \operatorname{int}(\mathbf{x})$ *then* $f(x) = 0$ *has a unique solution in* $\mathbf{x}$. *If* $\mathbf{N}(\mathbf{x}) \cap \mathbf{x} = \emptyset$ *then there are no zeros of* f *in* $\mathbf{x}$.

The elementary proof of the above theorem is given in the appendix for the completeness and in order to give the reader an idea of what kind of mathematics is involved when we use interval computations to rigorously prove the existence and uniqueness of zeros.

The interval Newton operator can be used only when the interval matrix $f'(\mathbf{x})$ is regular, i.e., composed of nonsingular matrices. The following two operators can be used for a wider class of systems.

2.3 Krawczyk and Hansen–Sengupta operators

Krawczyk operator is defined as

$$\mathbf{K}(\mathbf{x}) = x_0 - C f(x_0) - (C f'(\mathbf{x}) - I)(\mathbf{x} - x_0), \tag{3}$$

where x_0 is an arbitrary point belonging to $\mathbf{x}$ (usually one uses the center of $\mathbf{x}$) and C is a preconditioning matrix. It is usually chosen as the inverse of $f'(x_0)$.

Hansen–Sengupta operator is defined as

$$\mathbf{H}(\mathbf{x}) = x_0 + \Gamma(C\mathbf{D}f(\mathbf{x}), -C f(x_0), \mathbf{x} - x_0), \tag{4}$$

where Γ is the Gauss–Seidel operator [Neumaier, 1990]. For intervals $\mathbf{a}, \mathbf{b}, \mathbf{x}$ the Gauss–Seidel operator $\Gamma(\mathbf{a}, \mathbf{b}, \mathbf{x})$ is the tightest interval enclosing the set $\{x \in \mathbf{x} \colon ax =$

b for some $a \in \mathbf{a}, b \in \mathbf{b}\}$ and for interval matrix $\mathbf{A}$ and interval vectors $\mathbf{b}, \mathbf{x}$ the Gauss–Seidel operator $\Gamma(\mathbf{A}, \mathbf{b}, \mathbf{x})$ is defined by

$$\begin{aligned} \mathbf{y}_i &= \Gamma(\mathbf{A}, \mathbf{b}, \mathbf{x})_i \\ &= \Gamma\left(\mathbf{A}_{ii}, b_i - \Sigma_{k<i} \mathbf{A}_{ik} \mathbf{y}_k - \Sigma_{k>i} \mathbf{A}_{ik} \mathbf{x}_k, \mathbf{x}_i\right). \end{aligned} \tag{5}$$

For these two operators there are similar theorems on the existence and uniqueness of zeros as for the Newton operator (see [Neumaier, 1990]).

2.4 Existence of periodic orbits. Standard and global versions

The above three operators can be used to prove the existence of period-n cycles of f by applying the interval operator to the map $g = \mathrm{id} - f^n$. We shall call this technique a *standard* version of the method.

Another choice, which will be called a *global* version, is to apply the interval operator to the map $F : (\mathbb{R}^m)^n \mapsto (\mathbb{R}^m)^n$ defined by

$$[G(z)]_k = x_{(k+1) \bmod n} - f(x_k) \tag{6}$$

for $k = 0, \ldots, n-1$, where $z = (x_0, \ldots, x_{n-1})$. See that $G(z) = 0$ if and only if x_0 is a fixed point of f^n. In this method, the problem of existence of periodic orbits is translated to the problem of existence of zeros of a higher–dimensional function.

2.5 Finding all periodic orbits

In this study we are interested in finding for a given map all period-n cycles enclosed in a certain region A.

In order to find fixed points of f^n we use the combination of one of the interval methods described above and the generalized bisection (see also [Kearfott & Novoa, 1990]). First the region of interest is covered by m–dimensional intervals (the number of them increases with n). For each interval $\mathbf{x}$ the interval operator $\mathbf{N}(\mathbf{x})$ for the map g (standard method) or G (global method) is evaluated, where $\mathbf{N}$ stands for Newton, Krawczyk or Hansen–Sengupta operators. If $\mathbf{N}(\mathbf{x}) \subset \mathrm{int}(\mathbf{x})$ then there is exactly one fixed point of f^n in $\mathbf{x}$. If $\mathbf{N}(\mathbf{x}) \cap \mathbf{x} = \emptyset$ then there are no fixed points of f^n in $\mathbf{x}$. If none of these two conditions is fulfilled we divide the interval vector $\mathbf{x}$ into smaller parts and repeat the computations.

For the Newton operator we have to use a different non–existence stopping criterion. The reason is that we are not able to evaluate the interval Newton operator for each interval vector containing a point x such that $f'(x)$ is not invertible. Hence as the non–existence criterion we use the following condition: $\mathbf{N}(\mathbf{x}) \cap \mathbf{x} = \emptyset$ or $f^n(x) \cap \mathbf{x} = \emptyset$. The second part of the condition allows us to exclude regions for which the Jacobian matrix is singular. This is not necessary for the two other operators as for their evaluation we do not need to invert the interval matrix $f'(\mathbf{x})$.

Let us notice that none of the methods is capable of proving the existence of non-hyperbolic periodic orbit. If such a case is detected the procedure should as a result return also the interval vectors for which the method failed. Such instances are rare and in the examples considered, we have not found a single case like that. The uniqueness results in this case can no longer be proved. In order to prove the existence of non-hyperbolic orbits one may use purely topological methods based on the concept of topological index or its simple formulation going back to [Miranda, 1940] (see also [Neumaier, 1990]).

2.6 Reducing the dimension of the search space for the global version

The problem that arises, when we implement the global version, is the dimension of the space, where we are looking for periodic orbits. In order to find all period–n orbits of an m–dimensional map we have to search an mn–dimensional space.

In order to reduce the dimension of the search space we propose to use $\mathbb{R}^m$ as the search space. For the interval vector $\mathbf{x} \in \mathbb{R}^m$ we first produce the sequence $(\mathbf{x}_i)_{i=0}^{n-1}$, where $\mathbf{x}_i = f^i(\mathbf{x})$ and we set $\mathbf{z} = (\mathbf{x}_0, \ldots, \mathbf{x}_{n-1})$. Then we apply the global interval operator to $\mathbf{z}$. If the division is necessary we divide the m–dimensional interval $\mathbf{x}$, instead of mn–dimensional interval $\mathbf{z}$. Although some of the components of $\mathbf{z}$ generated from $\mathbf{x}$ using the procedure described above may by large (due to the wrapping effect and positive Lyapunov exponents of f if f is chaotic) it appears that this method is superior to all the other methods.

2.7 Further modifications

In order to speed up the algorithm we add two modifications.

The first modification uses the fact that we search for periodic solutions enclosed in A. For the interval $\mathbf{x}$ under consideration we compute several forward and backward (if the map is invertible) iterations. If for some positive i the image $f^i(\mathbf{x})$ or the inverse $f^{-i}(\mathbf{x})$ lies outside A than there is no periodic orbit in $\mathbf{x}$, which is entirely enclosed in A. Obviously if A is the trapping region for the map ($f(A) \subset A$) it makes no sense to check the forward iterates as for $\mathbf{x} \cap A \neq \emptyset$ we have $f^n(\mathbf{x}) \cap A \neq \emptyset$ for all $n > 0$.

The second modification is possible because we are searching for periodic orbits. As before we compute $f^i(\mathbf{x})$ for positive and negative i. If any of these iterations is enclosed in the region for which the algorithm was completed then we can skip the interval $\mathbf{x}$, as there are no new periodic orbits in $\mathbf{x}$.

3 Invariant Part and Nonwandering Part

Our main goal is to find all periodic orbits enclosed in the region A. In many cases it is possible to reduce the computation time by removing parts of the region A which cannot contain periodic orbits. In this section, we develop methods for reducing the search area for periodic orbits based on the notions of invariant and nonwandering part of a set.

For $A \subset \mathbb{R}^m$ we define the *invariant part* of A under the map f as

$$\mathrm{Inv}(A) = \{x \colon \exists (x_k)_{k=-\infty}^{\infty} \text{ such that } x_0 = x,\ x_k \in A \text{ and } x_{k+1} = f(x_k) \text{ for all } k\}. \quad (7)$$

We say that a set A is a *trapping region* for f if $f(A) \subset A$. If A is a trapping region the *invariant part* of A can be also defined as

$$\mathrm{Inv}(A) = \bigcap_{n \geq 0} f^n(A). \tag{8}$$

3.1 Invariant sets

Here we describe the algorithm finding for a given set A a possibly small set enclosing $\mathrm{Inv}(A)$. The set found will be the union of boxes (called interval vectors when the procedure is implemented using computer interval arithmetic).

Let us choose positive real numbers ε_i, $i = 1, 2, \dots, m$. Let $\varepsilon = (\varepsilon_1, \varepsilon_2, \dots, \varepsilon_m)$. Let us call an ε*–box* a set of the form

$$[k_1\varepsilon_1, (k_1+1)\varepsilon_1] \times [k_2\varepsilon_2, (k_2+1)\varepsilon_2] \times \cdots \times [k_m\varepsilon_m, (k_m+1)\varepsilon_m], \tag{9}$$

where k_i are integer numbers. Let $V = \{\mathbf{v}_i\}$ be a set of boxes. By $|V|$ we will denote the sum of all boxes in V ($|V| = \bigcup \mathbf{v}_i$).

Boxes of the form (9) are very well suited for interval computations. First by changing ε one may achieve arbitrary good approximation of representing a given set by the set of ε–boxes. In a computer program when ε is fixed an ε–box can be represented as a sequence of integers $(k_1, k_2, \dots, k_m)$. This makes it easier for the program to check whether a particular ε–box belongs to a set of boxes.

First let us assume that the set A is the sum of a finite number of ε–boxes, i.e., $V = \{\mathbf{v}_i\}$ is a set of boxes and $A = |V| = \bigcup \mathbf{v}_i$).

The following procedure from the set of boxes V removes those which has empty intersection with the invariant part of A. It is convenient to express the algorithm in the language of the graph theory. We create the directed graph $G = (V, E)$ where vertices $\mathbf{v}_i \in V$ are boxes and the edges correspond to the possibility of going from one box to another under the action of f. In order to create the set of edges for each box $\mathbf{v}_i$ we evaluate $f(\mathbf{v}_i)$ and we add edge e_{ij} if $f(\mathbf{v}_i) \cap \mathbf{v}_j \neq \emptyset$. Below we describe the algorithm in terms of a simple model language with clear meaning of syntax.

```
procedure ReduceInvariantPart(V)
  E ← the set of edges (e_{i,j} ∈ E if f(v_i) ∩ v_j ≠ ∅);
  repeat
    Improved ← FALSE;
    for all v_i ∈ V do begin
      if ∀j e_ij ∉ E or ∀j e_ji ∉ E then begin
        remove v_i and all edges incident with v_i from the graph;
        Improved ← TRUE;
      end
    end
  until not Improved;
end of ReduceInvariantPart
```

In the above procedure the box $\mathbf{v}_i$ is removed if $f(\mathbf{v}_i) \cap \mathbf{v}_j = \emptyset$ for all j (the box $\mathbf{v}_i$ is not the beginning of any edge in the graph) or if $f(\mathbf{v}_j) \cap \mathbf{v}_i = \emptyset$ for all j (the box

$\mathbf{v}_i$ is not the end of any edge in the graph). We proceed until no more boxes can be removed.

In order to compute the invariant part of an arbitrary set A we first choose $\varepsilon = (\varepsilon_1, \ldots, \varepsilon_m)$ and cover A by ε–boxes. We call the procedure `ReduceInvariantPart` to remove boxes which has empty intersection with $\mathrm{Inv}(A)$. Then we refine the division of the remaining boxes and call the procedure `ReduceInvariantPart` again. We continue until we reach a prescribed accuracy. Subsequent calls of `ReduceInvariantPart` and refining the division is actually better solution then starting with the accuracy we want to achieve and calling the procedure `ReduceInvariantPart` once only. This latter choice would lead to a huge number of vertices in the graph and make the procedure very slow. The procedure performing this task is presented below.

```
procedure FindInvariantPart(A,V)
  set ε_0; (desired accuracy)
  set ε = (ε_1, ε_2, ..., ε_m); (defining the initial division into boxes)
  V ← the set of ε-boxes covering A;
  ReduceInvariantPart(V);
  while (min(ε) < ε_0) do begin
    ε ← ε/2;
    V ← the set of ε-boxes covering |V| ∩ A;
    ReduceInvariantPart(V);
  end
end of FindInvariantPart
```

The following lemma states that given A the above procedure returns the set of boxes containing the invariant part of A.

Lemma 1. *Let V be the set of boxes returned by the procedure* `FindInvariantPart`*. Then*

$$\mathrm{Inv}(A) \subset |V| = \bigcup \mathbf{v}_i. \tag{10}$$

Proof. We show that the condition

$$\mathrm{Inv}(A) \subset |V| \tag{11}$$

is fulfilled during the whole course of the procedure. At the beginning by the construction $A \subset |V|$ and since $\mathrm{Inv}(A) \subset A$ the condition (11) is true. During the procedure we remove the box $\mathbf{v}_i$ if $f(\mathbf{v}_i) \cap \mathbf{v}_j = \emptyset$ for all $\mathbf{v}_j \in V$ or $f(\mathbf{v}_j) \cap \mathbf{v}_i = \emptyset$ for all $\mathbf{v}_j \in V$.

Let us consider the first case, i.e., $f(\mathbf{v}_i) \cap \mathbf{v}_j = \emptyset$ for all $\mathbf{v}_j \in V$. Let us choose $x \in \mathbf{v}_i$. It follows that $f(x) \cap |V| = \emptyset$. Since $\mathrm{Inv}(A) \subset |V|$ we have $f(x) \notin \mathrm{Inv}(A)$. From the property of the invariant part ($x \in \mathrm{Inv}(A) \Rightarrow f(x) \in \mathrm{Inv}(A)$) we obtain $x \notin \mathrm{Inv}(A)$ for all $x \in \mathbf{v}_i$. Finally $\mathbf{v}_i \cap \mathrm{Inv}(A) = \emptyset$ and $\mathrm{Inv}(A) \subset |V| \setminus \mathbf{v}_i$.

Now let us assume that $f(\mathbf{v}_j) \cap \mathbf{v}_i = \emptyset$ for all $\mathbf{v}_j \in V$. It follows that $x \notin f(|V|)$ for all $x \in \mathbf{v}_i$ and hence $x \notin f(\mathrm{Inv}(A))$ for all $x \in \mathbf{v}_i$. Since the implication $x \in \mathrm{Inv}(A) \Rightarrow x \in f(\mathrm{Inv}(A))$ is true, we have $x \notin \mathrm{Inv}(A)$ for all $x \in \mathbf{v}_i$ and in consequence $\mathrm{Inv}(A) \subset |V| \setminus \mathbf{v}_i$.

We have shown that in both cases $\mathrm{Inv}(A) \subset |V| \setminus \mathbf{v}_i$, so after removing $\mathbf{v}_i$ from V the condition (11) still holds. □

3.2 Nonwandering component

Previously we have described the method how to obtain a rigorous enclosure of the set $\mathrm{Inv}(A)$. The invariant part of the trapping region may contain stable and unstable manifolds of fixed or periodic points. The so-called nonwandering component is perhaps more important to the study of long–term behavior. Fixed points and closed orbits are important in the study of dynamical systems, since they represent stationary or repeatable behavior. A generalization of these sets is the nonwandering set. A point x is called *nonwandering* for the map f if for any neighborhood U of x there exists $n > 0$ such that $f^n(U) \cap U \neq \emptyset$. The set of nonwandering points is closed and it contains the closure of the set of fixed points and periodic orbits. For a given set A we define the *nonwandering part* of A as the set of nonwandering points of the map $f|\mathrm{Inv}(A)$.

We can easily adapt the procedure `ReduceInvariantPart` to remove from V boxes having empty intersection with the nonwandering part of $|V|$. We modify the procedure by adding one more condition under which the box may be removed from the graph. If for a given ε–box there is no closed path of edges going through this box then this box contains wandering points only and must lie completely outside the nonwandering part. We may then remove this box from the graph. The problem of finding vertices not belonging to any closed loops is equivalent to searching for strongly connected components in a graph. This is a standard problem in algorithmic graph theory and has a very fast solution, which operates in linear time [Gibbons, 1985]. The algorithm for removing boxes not belonging to the nonwandering part of a set of boxes is given below.

```
procedure ReduceNonwanderingPart(V)
  E ← the set of edges (e_{i,j} ∈ E if f(v_i) ∩ v_j ≠ ∅);
  repeat
    Improved ← FALSE;
    for all v_i ∈ V do begin
      if ∀j  e_ij ∉ E or ∀j  e_ji ∉ E then begin
      or v_i does not belong to any closed path then begin
        remove v_i and all edges incident with v_i from the graph;
        Improved ← TRUE;
      end
    end
  until not Improved;
end of ReduceNonwanderingPart
```

The procedure `FindNonwanderingPart` for finding the enclosure of nonwandering part of an arbitrary set is the same as the procedure `FindInvariantPart` except that it calls the procedure `ReduceNonwanderingPart` instead of `ReduceInvariantPart`. One can easily show that the set $|V|$ returned by this procedure contains the nonwandering part of A.

The above procedures can be implemented in a very fast and efficient way. The most time–consuming part is the generation of the connections in the graph. In subsequent sections, we apply these procedures for finding nonwandering component of the trapping regions for the Ikeda and Hénon maps. We will show that with these procedures one can significantly reduce the region, which needs to be checked in order to find all periodic orbits for the map.

3.3 Basins of attraction of stable periodic orbits

When studying periodic orbits for a particular system we may encounter a stable periodic orbit. A question, which arises, is what is its basin of attraction. We say that a periodic orbit $p = \{x_1, \dots, x_m\}$ is *asymptotically stable* if there is some neighborhood U of p such that $f^k(x) \in U$ for $k \geq 0$ and $f^k(x) \to p$ as $k \to \infty$ for all $x \in U$. A *basin of attraction* of a periodic orbit is a set of points which converge to this periodic orbit as time goes to infinity

$$\{x\colon f^k(x) \to p \text{ for } k \to \infty\}. \tag{12}$$

Let B and A be arbitrary sets and assume that $B \subset A$. The procedure `FindBasin` presented below returns the set of boxes V enclosed in the basin of attraction of B,

$$|V| \subset \{x\colon \exists n \geq 0 \quad f^n(x) \in B\}. \tag{13}$$

The search is limited to A, i.e., we check only boxes, which has non–empty intersection with A. At the beginning of the procedure V is the set of boxes enclosed in B and W if the set of boxes, which covers $A \setminus B$. We move a box $\mathbf{w}_i$ from W to V if this box or its image is enclosed in V. We continue until no more boxes can be moved from W to V. Then we refine the division of boxes and repeat computations until a prescribed accuracy is achieved.

```
procedure FindBasin(B,A,V)
  set ε₀;
  set ε = (ε₁,ε₂,...,εₘ);
  V ← ∅;
  repeat
    V ← the set of ε-boxes enclosed in B ∪ |V|;
    W ← the set of ε-boxes covering A \ (B ∪ |V|);
    repeat
      Improved ← FALSE;
      for all wᵢ ∈ W do begin
        if wᵢ ⊂ |V| or f(wᵢ) ⊂ |V| then
          move wᵢ from W to V;
          Improved ← TRUE;
        end
      end
    until Improved;
    ε ← ε/2;
  until (min(ε) < ε₀);
```

```
end of FindBasin
```

The above procedure describes the basic idea for finding a subset of A of points, which eventually visit B. Several refinements are possible. One may for example use higher iterations of f as a test condition for moving $\mathbf{w}_i$ from W to V. Another modification is to evaluate $f(\mathbf{w}_i)$ after dividing $\mathbf{w}_i$ into smaller boxes. This helps to avoid the wrapping effect.

Now we explain how to use the above algorithm to find the basin of attraction of a stable periodic orbit. Assume that p is an asymptotically stable periodic orbit and we want to find the intersection of its basin of attraction with a given set A. Since the orbit is asymptotically stable it is easy to find a neighborhood U of p which is a trapping region for the map. We use this set as a starting point for our procedure. To find intersection of A with the basin of attraction of p we call the procedure `FindBasin` with parameters U and A. This allows us to obtain rigorous approximation of the basin of attraction. It is rigorous in the sense that the union of the set of boxes V returned by the procedure is enclosed in the basin of attraction of p. This information can be used for many different purposes. One of them is search for periodic orbits. It is clear that there is no other periodic orbits of any period within the basin of attraction of p. Hence, if we locate the stable periodic orbit we can exclude points belonging to its basin of attraction from search for any other periodic orbits.

In the next part of the paper we use the above procedure for finding basin of attraction of the stable period–1 orbit for the Ikeda map.

4 Hénon Map

As a first example, we consider the Hénon map defined by the following equation [Hénon, 1976]

$$h(x, y) = (1 + y - ax^2, bx), \tag{14}$$

where $a = 1.4$ and $b = 0.3$ are the "classical" parameter values for which the famous Hénon attractor is observed.

It is well known [Hénon, 1976] that the set Ω defined as a quadrangle $ABCD$, where $A = (-1.33, 0.42)$, $B = (1.32, 0.133)$, $C = (1.245, -0.14)$ and $D = (-1.06, -0.5)$ is a trapping region for the Hénon map, i.e. $h(\Omega) \subset \Omega$. In our study we search for periodic solution in the trapping region Ω, which encloses the strange attractor observed numerically. The trapping region Ω and a trajectory of the Hénon map are shown in Fig. 1.

It can be easily checked that there are two fixed points for the Hénon map:

$$P_1 = (x_1, bx_1), \quad P_2 = (x_2, bx_2). \tag{15}$$

where

$$x_{1,2} = \frac{b - 1 \pm \sqrt{(1-b)^2 + 4a}}{2a}$$

Both of then are unstable. The point P_1 is located inside the trapping region while P_2 lies outside (compare Fig. 1).

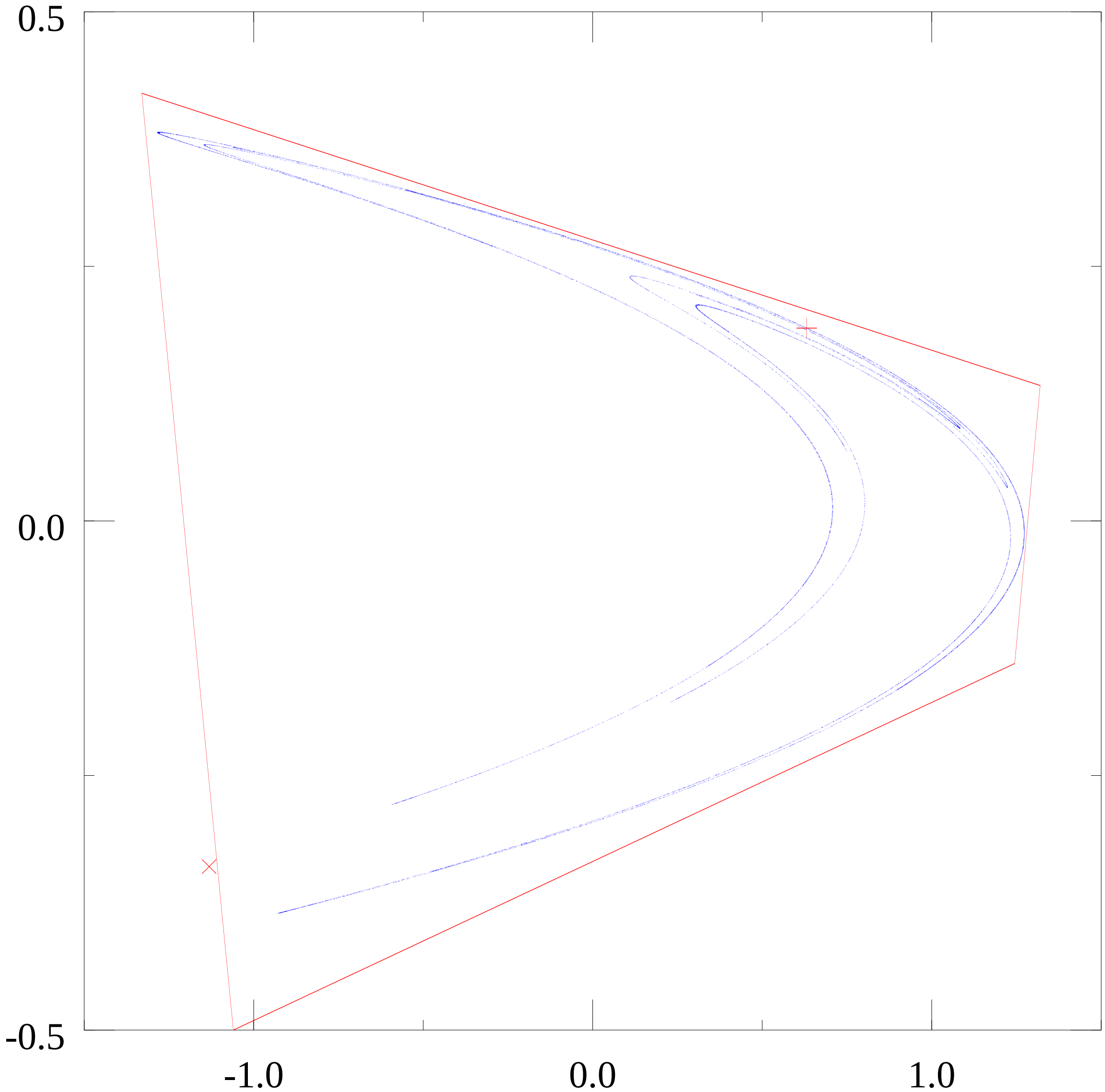

Figure 1: Trajectory of the Hénon map consisting of 20000 points and the trapping region Ω, unstable fixed points: inside the trapping region $(+)$ and outside the trapping region $(\times)$.

	Invariant part		Nonwandering part	
n	box #	area	box #	area
1	22	1.83	20	1.67
2	51	1.06	48	1.00
3	137	0.714	118	0.615
4	325	0.423	278	0.362
5	776	0.253	660	0.215
6	1892	0.154	1531	0.125
7	4577	0.0931	3387	0.0689
8	10464	0.0532	7804	0.0397
9	24768	0.0315	18665	0.0237
10	59581	0.0189	44817	0.0142
11	141426	0.0112	107938	0.00858

Table 1: The number of ε–boxes covering the invariant part and nonwandering part of the rectangle $[-1.5, 1.5] \times [-0.5, 0.5]$ and the area of the boxes, for given n $\varepsilon = (1/(2^n), 1/(3 \cdot 2^n))$.

4.1 Invariant part and nonwandering part

First let us find invariant part and nonwandering part of the rectangle $[-1.5, 1.5] \times [-0.5, 0.5]$ enclosing the trapping region Ω and the unstable fixed point P_2.

We find sets of ε–boxes covering the invariant part and nonwandering part for $\varepsilon = (1/2^n, 1/(3{\cdot}2^n))$, $n = 1, 2, \ldots, 11$. We also compute the area of the region obtained. The results are summarized in Table 1. The area for $n = 11$ of the region containing the nonwandering part is smaller than 0.0086. Hence using the representation of the nonwandering region by ε–boxes we can reduce the search region considerably (the area of the initial rectangle is 3).

The results obtained for invariant and nonwandering parts are shown in Fig. 2 and Fig. 3 respectively. Using different shades we plot results for different values of ε with darker color meaning finer division — larger n (in black we plot the results obtained for $n = 11$). One can clearly see that the enclosure of the invariant part contains the chaotic attractor, the unstable fixed point P_2 and the connection between these two sets. The enclosure of the nonwandering part is smaller and has two components. One contains the chaotic attractor while the second (very small) contains the unstable fixed point. We were able to break the connection between these two sets and removed the part of the unstable manifold of the fixed point P_2 from the enclosure of the nonwandering part.

4.2 Periodic orbits

In this section, we test the interval methods for finding periodic orbits described previously. First, we compare five versions of the interval Newton method: standard version (Newton Standard), standard version with modifications (Newton Standard +), global version with the search space $\mathbb{R}^2$ (Newton Global), global version with the

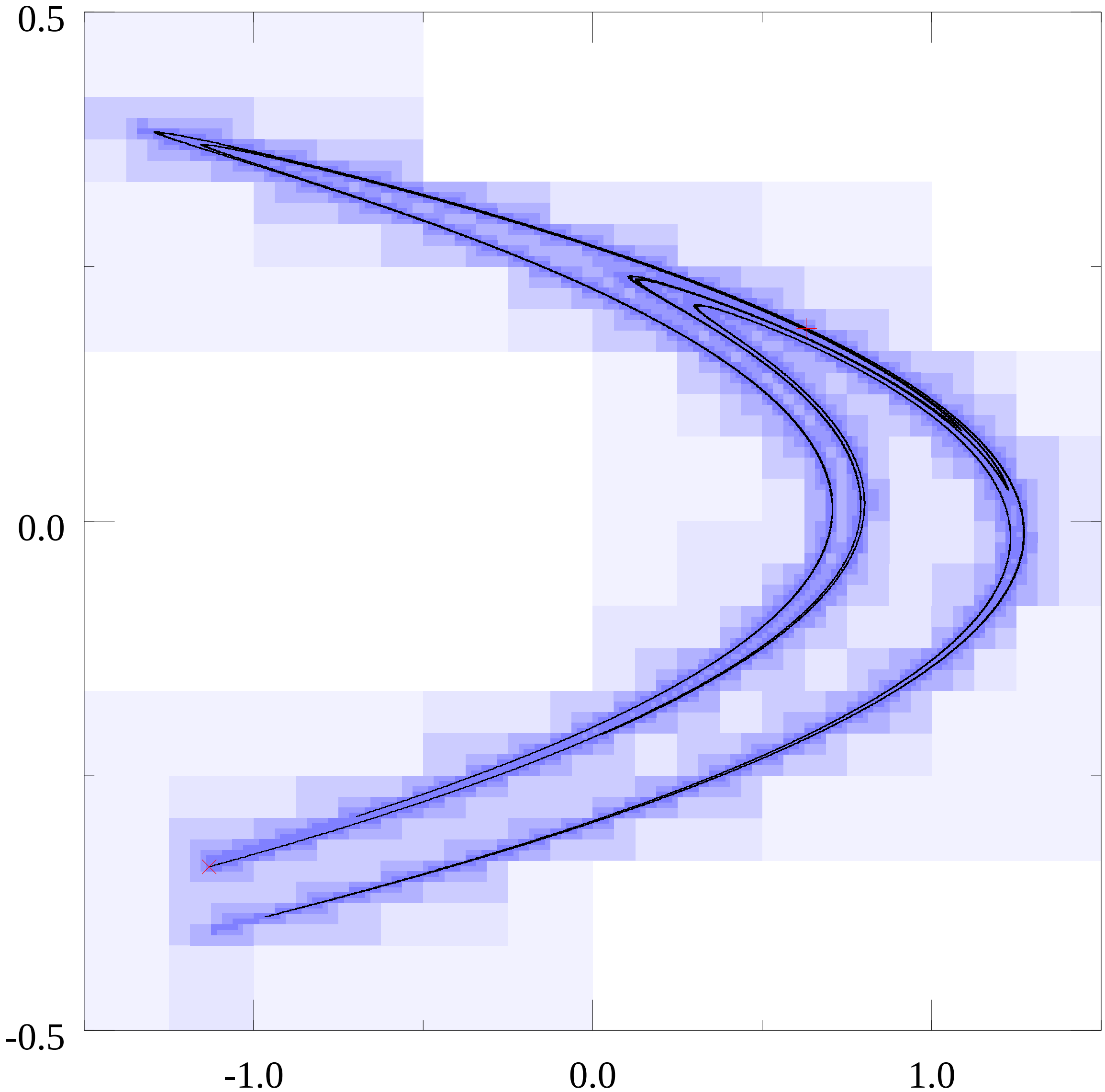

Figure 2: Hénon map, invariant part of the region $[-1.5, 1.5] \times [-0.5, 0.5]$, approximations of the invariant part obtained for different ε are plotted using different shades, unstable fixed points: inside the trapping region $(+)$ and outside the trapping region $(\times)$.

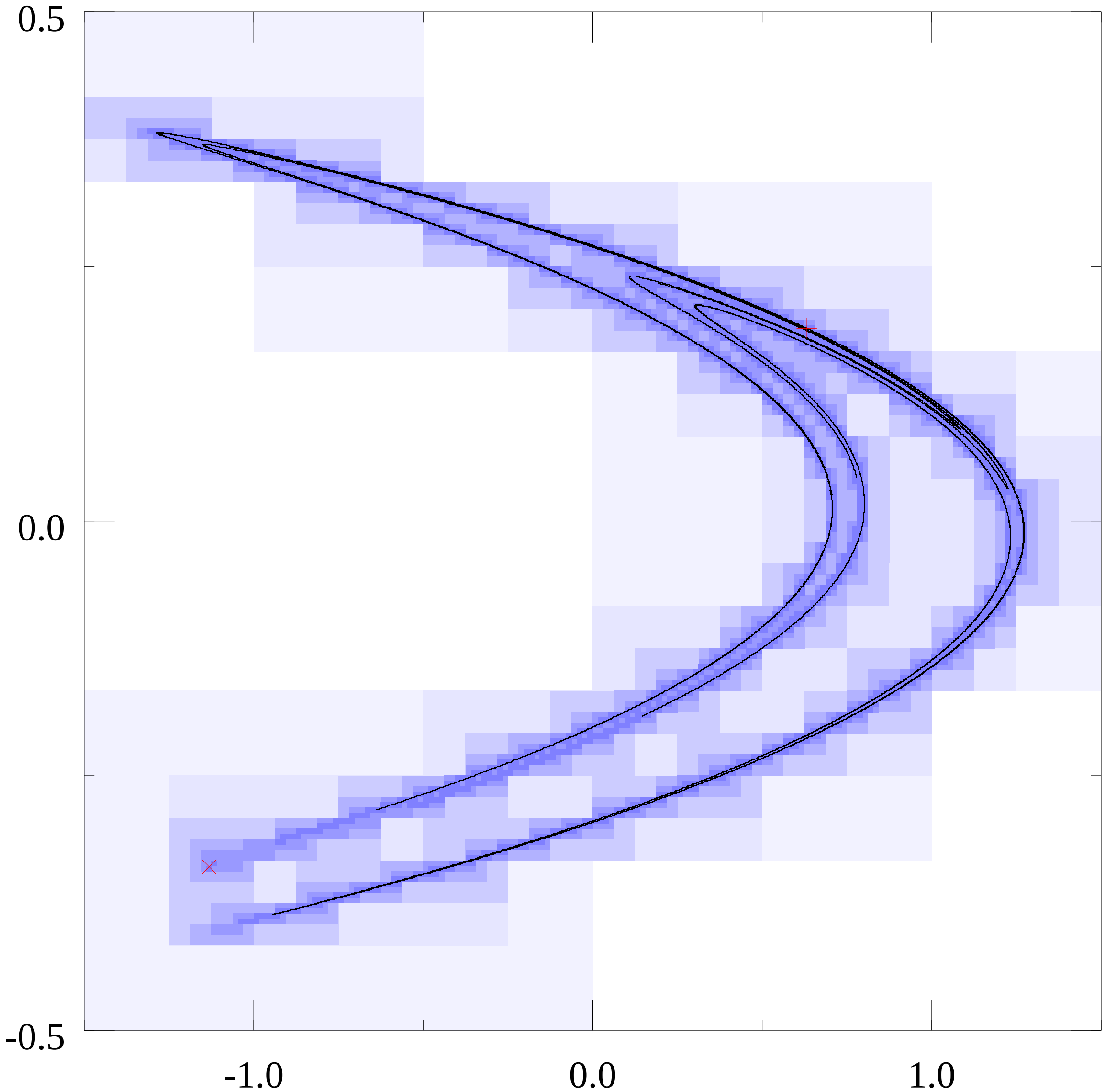

Figure 3: Hénon map, nonwandering part of the rectangle $[-1.5, 1.5] \times [-0.5, 0.5]$, unstable fixed points: inside the trapping region (+) and outside the trapping region ($\times$).

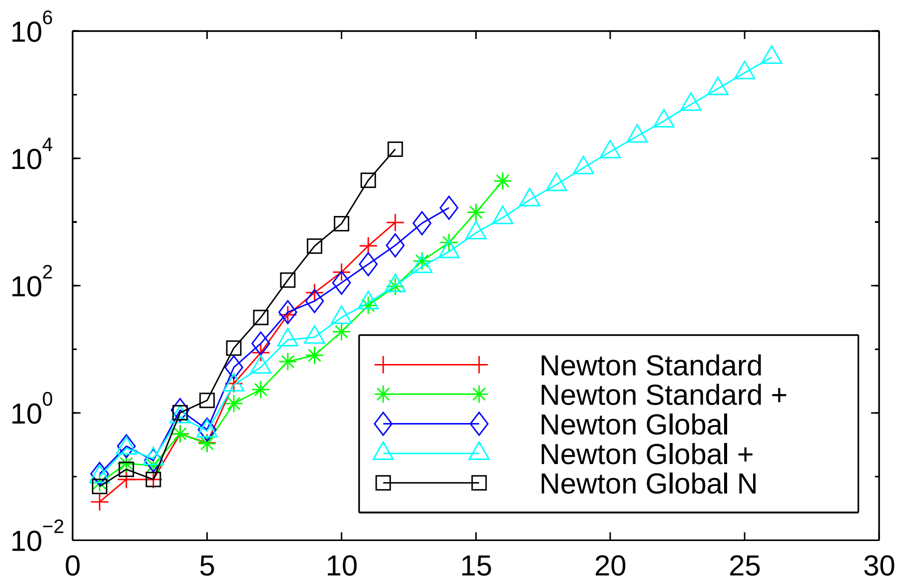

Figure 4: Computation time needed to find all period–n cycles using different versions of the interval Newton method: standard version, standard version with modifications, global version, global version with modifications and global version with $\mathbb{R}^{2n}$ search space.

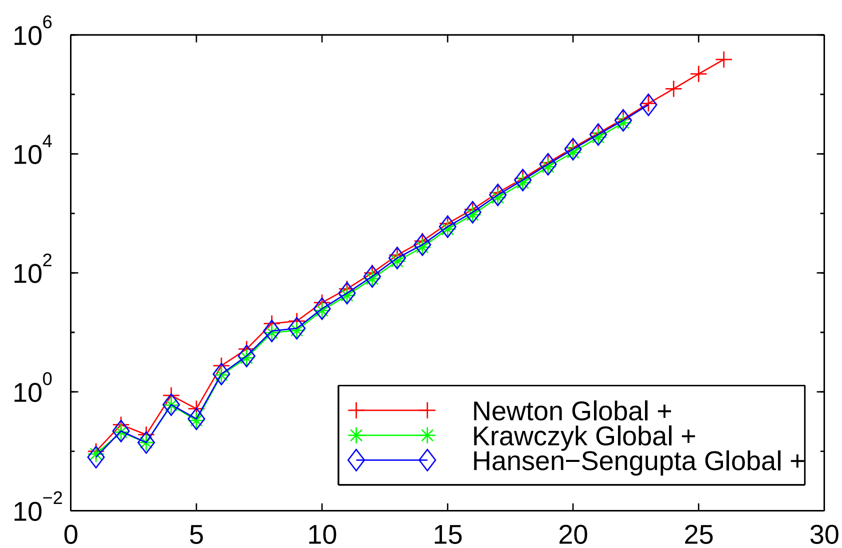

Figure 5: Computation time needed to find all period–n cycles using Newton, Krawczyk and Hansen–Sengupta methods.

search space $\mathbb{R}^2$ and with modifications (Newton Global +) and global version with $\mathbb{R}^{2n}$ search space (Newton Global N). In Fig. 4 we plot the computation time necessary to find all period–n cycles. For $n \leq 3$ the standard Newton method is the fastest. For $4 \leq n \leq 12$ the standard interval Newton method with modifications is the quickest one. It is not possible however to use the standard Newton method for finding all longer orbits. It appears that the method fails to find all periodic orbits with period n for $n > 17$. For $n = 18$ there are some periodic points x for which one cannot check the assumption $\mathbf{N}(\mathbf{x}) \subset \mathbf{x}$ for any interval vector $\mathbf{x} \ni x$. This is due to the wrapping effect, which causes that $\mathbf{D}h^n(\mathbf{x})$ has a very large diameter [Galias, 1998a]. For $N \geq 13$ the global version with reduced search space and other improvements is better.

It is interesting to note that the global version with search space $\mathbb{R}^{2n}$ is the worst one. Although many rectangles can be excluded before evaluation of the interval operator, the algorithm is very slow. It is even slower than the algorithm based on the standard Newton operator and hence of not much use.

In Fig. 5 we show the computation time for global versions of Newton, Krawczyk and Hansen–Sengupta methods. One can clearly see that there are no significant differences in computation time between these three methods.

Using the Krawczyk method which is slightly better than the two other methods we have found all periodic orbits with period $n \leq 30$. The periodic orbits found are plotted in Fig. 6. The results are summarized in Table 2, where we give the number Q_n of periodic orbits with period n, the number P_n of fixed points of h^n, estimation of topological entropy, and the number of rectangles into which the initial region was divided in order to find all periodic orbits. In particular, we have proved that there are no period–3 and period–5 orbits for the Hénon map within the trapping region. We have proved that there are exactly 109033 periodic orbits with period $n \leq 30$ and there are 3065317 points belonging to these orbits. These unstable periodic points shown in Fig. 7 give very good approximation of the Hénon attractor.

In Fig. 7 one can see small regions of the attractor not visited by periodic orbits found. Knowing the positions of periodic orbits, we can study an interesting problem how well the periodic orbits fill the attractor. In Table 3 we collect several numbers which give some insight into this problem. D_c and D_e describe the performance of the interval method. D_c is the minimum diameter of the interval for which uniqueness of period–n orbit was proved. We want this number to be as large as possible so we do not need to divide the search area in a very fine way to find all periodic orbits. It cannot be however larger that the distance between the closest period–n points. D_e is the maximum diameter of interval for which the existence was proved. This number describes the accuracy of the position of periodic orbit found. Clearly the accuracy degrades with n. $D_{\min}$, $D_{\max}$, and D_{av} describe how well periodic orbits fill the attractor. For each period–n point we find its closest neighbor and we define $D_{\min}$, $D_{\max}$, and D_{av} as the minimum, maximum, and average distance from the closest neighbor. The smaller $D_{\min}$ is the more difficult it is to find all periodic orbits as we need to divide the search region into smaller rectangles, as the existence theorem cannot work if there are two or more periodic points within a given rectangle. The value of $D_{\min} = 8.5 \cdot 10^{-8}$ for $n = 27$ means that some period–27 points are located very close to each other and we need a very fine division of the search area in order

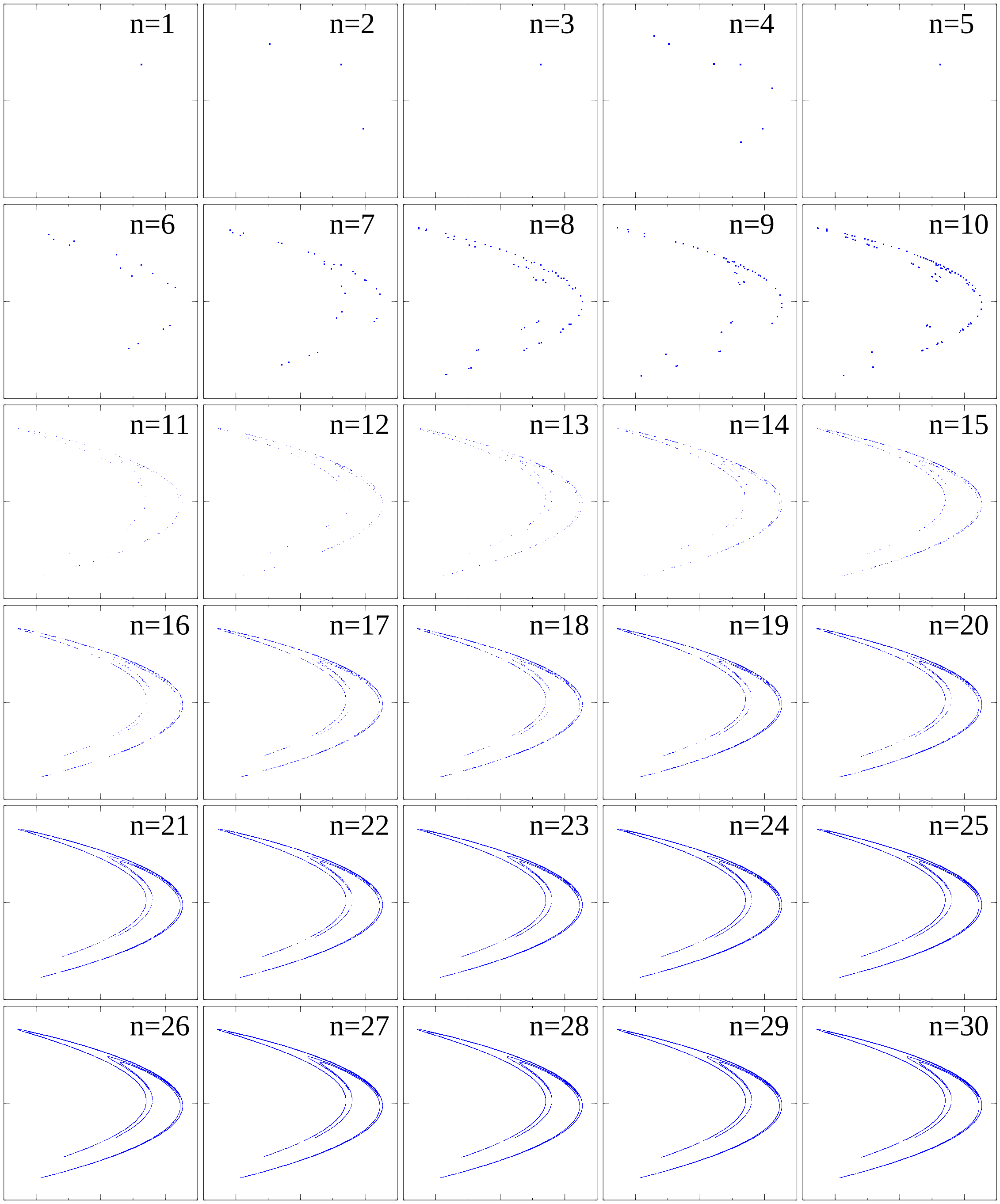

Figure 6: Period-n cycles of the Hénon map for $n = 1, \ldots, 30$ within the trapping region.

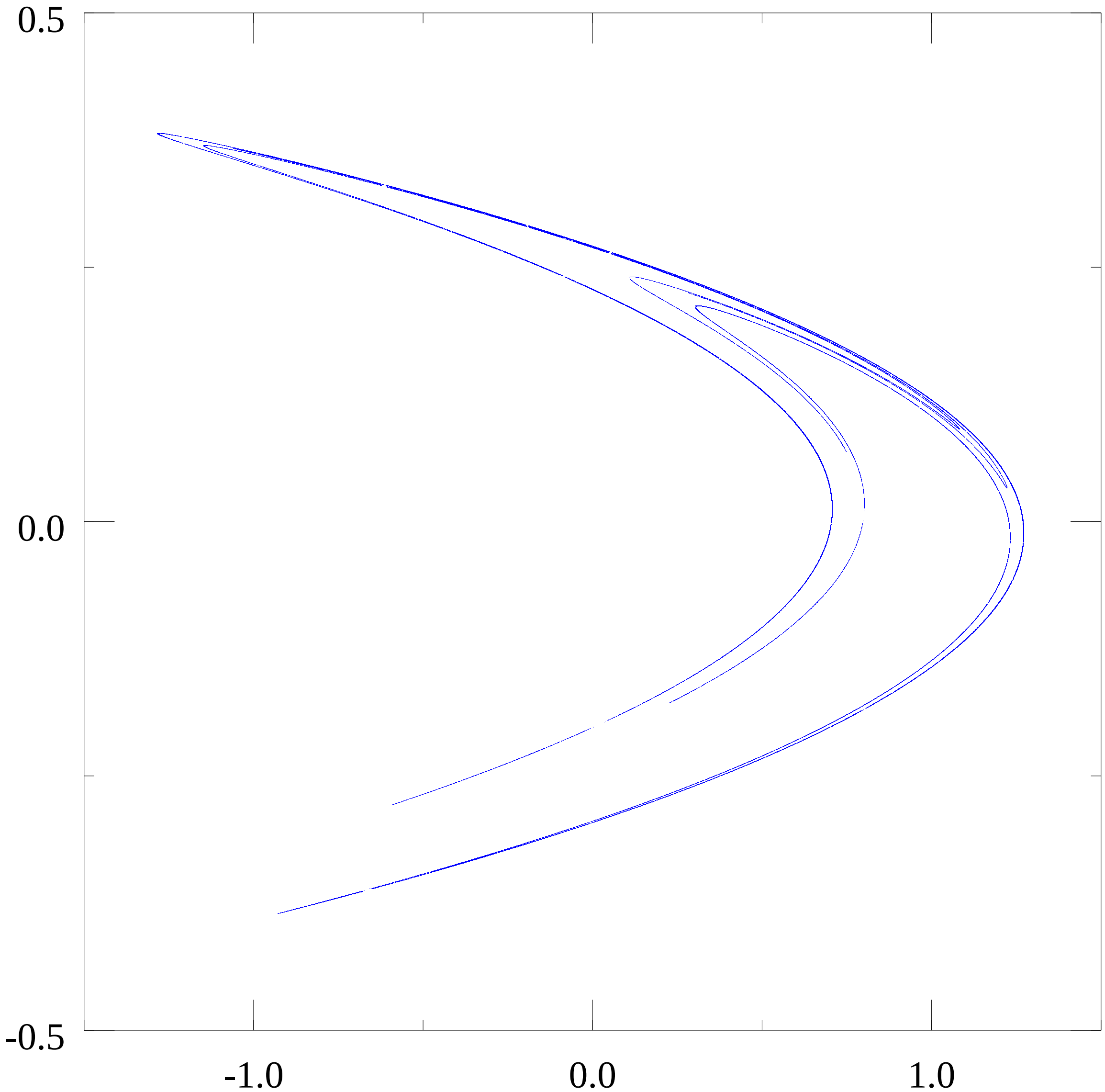

Figure 7: Cycles within the trapping region of the Hénon map with period $n = 1, \ldots, 30$.

n	Q_n	P_n	$\mathrm{Q}_{\le n}$	$\mathrm{P}_{\le n}$	H_n	rectangles
1	1	1	1	1	0.00000	9
2	1	3	2	3	0.54931	21
3	0	1	2	3	0.00000	41
4	1	7	3	7	0.48648	101
5	0	1	3	7	0.00000	89
6	2	15	5	19	0.45134	205
7	4	29	9	47	0.48104	285
8	7	63	16	103	0.51789	569
9	6	55	22	157	0.44526	737
10	10	103	32	257	0.46347	1149
11	14	155	46	411	0.45849	1521
12	19	247	65	639	0.45912	2457
13	32	417	97	1055	0.46408	4093
14	44	647	141	1671	0.46231	5973
15	72	1081	213	2751	0.46571	9653
16	102	1695	315	4383	0.46471	16281
17	166	2823	481	7205	0.46739	26273
18	233	4263	714	11399	0.46432	43545
19	364	6917	1078	18315	0.46535	71657
20	535	10807	1613	29015	0.46440	121181
21	834	17543	2447	46529	0.46535	199889
22	1225	27107	3672	73479	0.46398	333625
23	1930	44391	5602	117869	0.46525	560725
24	2902	69951	8504	187517	0.46481	961981
25	4498	112451	13002	299967	0.46521	1584185
26	6806	177375	19808	476923	0.46485	2670517
27	10518	284041	30326	760909	0.46507	4346609
28	16031	449519	46357	1209777	0.46485	7346653
29	24740	717461	71097	1927237	0.46495	12264301
30	37936	1139275	109033	3065317	0.46486	21058121

Table 2: Periodic orbits for the Hénon map. Q_n — number of periodic orbits with period n, P_n — number of fixed points of h^n, $\mathrm{Q}_{\le n}$ — number of periodic orbits with period smaller or equal to n, $\mathrm{P}_{\le n}$ — number of fixed points of h^i for $i \le n$, $\mathrm{H}_n = n^{-1}\log(\mathrm{P}_n)$ — estimation of topological entropy based on P_n.

n	P_n	D_c	D_e	D_{min}	D_{max}	D_{aver}
1	1	$7.2\cdot10^{-1}$	$4.5\cdot10^{-16}$	—	—	—
2	3	$9.1\cdot10^{-2}$	$7.8\cdot10^{-16}$	0.478	1.1120	0.69
3	1	$9.1\cdot10^{-2}$	$6.7\cdot10^{-16}$	—	—	—
4	7	$1.2\cdot10^{-2}$	$1.2\cdot10^{-15}$	0.235	0.4136	0.31
5	1	$3.2\cdot10^{-2}$	$7.8\cdot10^{-16}$	—	—	—
6	15	$3.8\cdot10^{-3}$	$1.4\cdot10^{-15}$	0.063	0.1770	0.11
7	29	$1.3\cdot10^{-3}$	$2.0\cdot10^{-15}$	0.016	0.1276	0.062
8	63	$2.9\cdot10^{-4}$	$5.4\cdot10^{-15}$	$5.4\cdot10^{-3}$	0.1032	0.041
9	55	$1.5\cdot10^{-4}$	$1.1\cdot10^{-14}$	$1.7\cdot10^{-3}$	0.1110	0.033
10	103	$1.5\cdot10^{-4}$	$6.0\cdot10^{-15}$	$2.0\cdot10^{-3}$	0.1183	0.024
11	155	$4.9\cdot10^{-5}$	$7.5\cdot10^{-15}$	$9.6\cdot10^{-4}$	0.0699	0.017
12	247	$5.2\cdot10^{-5}$	$7.0\cdot10^{-15}$	$5.0\cdot10^{-4}$	0.0498	0.011
13	417	$7.5\cdot10^{-6}$	$2.7\cdot10^{-14}$	$3.8\cdot10^{-4}$	0.0519	0.0079
14	647	$6.0\cdot10^{-6}$	$6.9\cdot10^{-15}$	$2.4\cdot10^{-4}$	0.0299	0.0044
15	1081	$1.9\cdot10^{-6}$	$1.3\cdot10^{-14}$	$1.2\cdot10^{-4}$	0.0237	0.0034
16	1695	$7.4\cdot10^{-7}$	$2.9\cdot10^{-14}$	$8.6\cdot10^{-5}$	0.0235	0.0021
17	2823	$7.0\cdot10^{-7}$	$1.7\cdot10^{-14}$	$3.9\cdot10^{-5}$	0.0210	0.0015
18	4263	$7.8\cdot10^{-8}$	$1.2\cdot10^{-13}$	$8.9\cdot10^{-6}$	0.0214	0.0011
19	6917	$2.2\cdot10^{-7}$	$2.1\cdot10^{-14}$	$1.4\cdot10^{-5}$	0.0139	0.00077
20	10807	$1.6\cdot10^{-8}$	$1.5\cdot10^{-13}$	$3.7\cdot10^{-6}$	0.0138	0.00053
21	17543	$9.9\cdot10^{-9}$	$5.2\cdot10^{-14}$	$4.9\cdot10^{-6}$	0.0077	0.00038
22	27107	$4.9\cdot10^{-9}$	$2.7\cdot10^{-13}$	$5.5\cdot10^{-7}$	0.0109	0.00026
23	44391	$3.2\cdot10^{-9}$	$6.4\cdot10^{-14}$	$1.3\cdot10^{-6}$	0.0055	0.00018
24	69951	$1.4\cdot10^{-9}$	$1.4\cdot10^{-13}$	$3.2\cdot10^{-7}$	0.0047	0.00012
25	112451	$5.0\cdot10^{-10}$	$9.6\cdot10^{-14}$	$3.3\cdot10^{-7}$	0.0041	0.000086
26	177375	$2.2\cdot10^{-10}$	$9.2\cdot10^{-14}$	$1.2\cdot10^{-7}$	0.0026	0.000060
27	284041	$5.3\cdot10^{-11}$	$1.7\cdot10^{-13}$	$8.5\cdot10^{-8}$	0.0044	0.000041

Table 3: Short cycles for the Hénon map, D_c — diameter of interval for which uniqueness was proved, D_e — diameter of interval for which existence was proved, closest neighbor distance: D_{min}, D_{max}, D_{av}.

to find all periodic orbits. Large $D_{\max}$ indicates that there are period–n points well separated from other such points and this means that periodic points do not fill the attractor densely. $D_{\max}$ does not decrease as fast with n as one could expect (see for example $D_{\max}$ for $n = 22, \ldots, 27$). This corresponds to clearly visible gaps in Fig. 7.

4.3 Estimation of topological entropy

In this section we use the number of periodic orbits for the estimation of topological entropy of the Hénon map.

Topological entropy $\mathrm{H}(f)$ of a map f characterizes "mixing" of points by the map f. One of the equivalent definitions of topological entropy is based on the notion of (n, ε)–separated sets (see [Bowen, 1971]).

A set $E \subset X$ is called (n, ε)*–separated* if for every two different points $x, y \in E$, there exists $0 \leq j < n$ such that the distance between $f^j(x)$ and $f^j(y)$ is greater than ε. Let us define the number $s_n(\varepsilon)$ as the cardinality of a maximum (n, ε)–separated set:

$$s_n(\varepsilon) = \max\{\,\mathrm{card}\, E : E \ is \ (n, \varepsilon)\text{-separated}\,\}$$

The number

$$\mathrm{H}(f) = \lim_{\varepsilon \to 0} \limsup_{n \to \infty} \frac{1}{n} \log s_n(\varepsilon), \tag{16}$$

is called the *topological entropy* of the map f. The number of periodic orbits is closely related to the topological entropy. For axiom A diffeomorphisms we have

$$\mathrm{H}(f) = \lim_{n \to \infty} \frac{\log \mathrm{P}_n}{n}, \tag{17}$$

where P_n denotes the number of fixed points of f^n. It is also possible to use the number of periodic orbits for the estimation of topological entropy when there exists a symbolic dynamics for the map.

Using the existence of symbolic dynamics for h^7 one can prove that (compare [Zgliczyński, 1997, Galias, 1998*b*]):

$$\mathrm{H}(h) \geq \frac{1}{7} \log 2 > 0.099.$$

Similarly one can obtain the estimation of topological entropy based on the existence of symbolic dynamics for h^2 (compare [Galias, 1998*b*]):

$$\mathrm{H}(h) \geq \frac{1}{2} \log \frac{\sqrt{5} + 1}{2} > 0.24.$$

In Fig. 8(a) we plot in semilogarithmic scale the number P_n of fixed points of h^n as a function of n. One can see that for $n > 10$ the plot is almost linear, which indicates

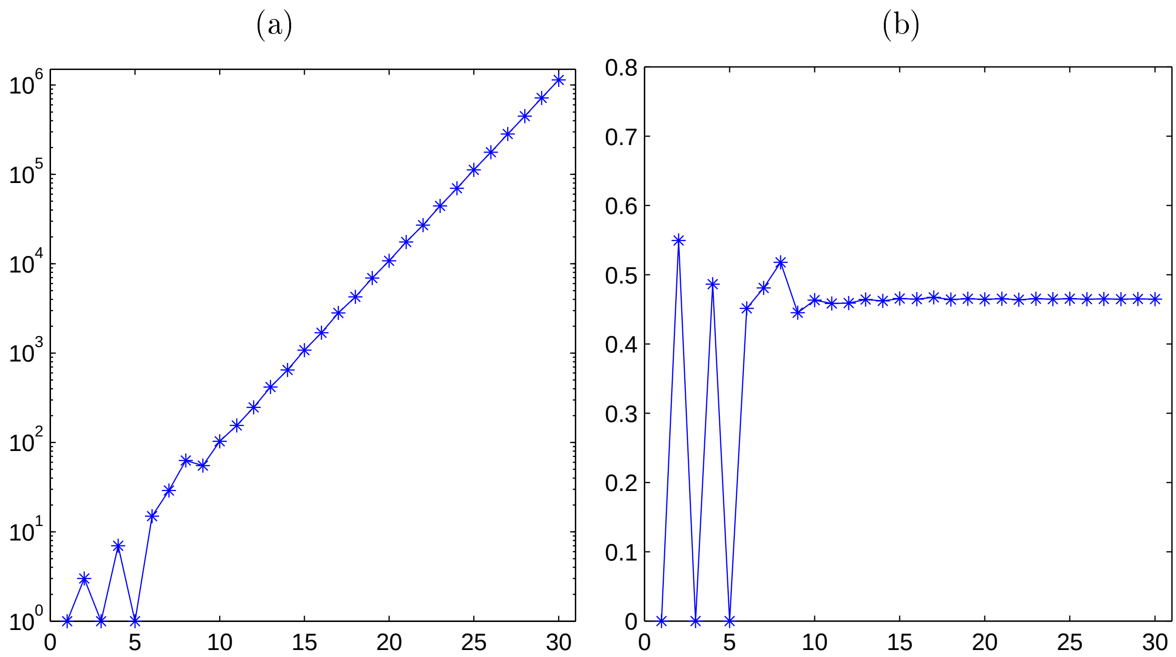

Figure 8: (a) The number of fixed points of h^n and (b) Estimation of topological entropy of the Hénon map based on the number of low–period cycles.

that the number P_n can be used for obtaining a good approximation of topological entropy. Here we use the formula

$$\mathrm{H}_n(h) = \frac{\log \mathrm{P}_n}{n} \tag{18}$$

as the approximation of topological entropy. The results are plotted in Fig. 8(b) (see also Table 2). One can see that $\mathrm{H}_n(h)$ is almost constant for $n \geq 10$. This lets us state the hypothesis that the topological entropy of the Hénon map is close to 0.465.

5 Ikeda Map

As a second example let us consider the Ikeda map [Hammel et al., 1985]

$$f(z) = p + B \exp\left(i\kappa - i\alpha/(1 + |z|^2)\right) z, \tag{19}$$

where $z = x + iy$ is a complex number. This map can be written as a two dimensional system in the following form:

$$f(x, y) = (p + B(x \cos t - y \sin t), B(x \sin t + y \cos t)), \tag{20}$$

where $t = t(x, y) = \kappa - \alpha/(1 + x^2 + y^2)$.

First let us observe that the ball $K = \mathrm{B}((p, 0), pB/(1 - B))$ is a trapping region for the map f ($f(K) \subset K$) [Hammel et al., 1985]. For $z \in K$ we have

$$|f(z) - p| \leq B|z| \leq B(p + \frac{pB}{1 - B}) = \frac{pB}{1 - B},$$

n	Invariant part		Nonwandering part	
	box #	area	box #	area
0	61	61.00	61	61.00
1	155	38.80	69	17.20
2	328	20.50	176	11.00
3	789	12.30	368	5.75
4	1971	7.70	1098	4.29
5	5392	5.27	3597	3.51
6	15399	3.76	11890	2.90
7	46604	2.84	39660	2.42
8	145346	2.22	131837	2.01

Table 4: The number of ε–boxes covering the invariant part and nonwandering part of the trapping region and sum of the area of the boxes for $\varepsilon = (1/2^n, 1/2^n)$.

and hence $f(z) \in K$.

It may be shown that all initial points are mapped to this trapping region in finite time and hence we may limit our analysis to the behavior of the system in the trapping region.

We consider the Ikeda map with the following parameter values: $p = 1$, $B = 0.9$, $\kappa = 0.4$ and $\alpha = 6$, for which in simulations a chaotic behavior is observed. A typical chaotic trajectory is shown in Fig. 9.

There are three fixed points of the map. They belong to the following interval vectors:

$$
\begin{aligned}
P_1 &\in (2.9721316179105^{71}_{38}, 4.145946421395^{91}_{87}),\\
P_2 &\in (0.5327546229407^{93}_{88}, 0.24689677271101^{49}_{12}),\\
P_3 &\in (1.114269614581^{43}_{39}, -2.2856944609861^{45}_{69}).
\end{aligned}
$$

The first fixed point is stable and the two others are unstable. P_2 belongs to the numerically observed chaotic attractor.

We have found sets of ε–boxes enclosing the invariant part and the nonwandering part of the trapping region. The results are shown in Fig. 10 and 11 respectively and summarized in Table 4. We plot the results for $\varepsilon = (1/2^n, 1/2^n)$ for $n = 0, \ldots, 8$ using different shades and black denoting the smallest set ($n = 8$).

The invariant part contains the stable fixed point, unstable periodic point, chaotic attractor and unstable manifold of P_3 connecting this point with the stable fixed point and the chaotic attractor. The area of the region obtained is 2.22.

The nonwandering part is smaller than the invariant part. Its area is 2.01. It does not contain the heteroclinic orbit connecting the unstable and stable fixed points. We were not able however to break the connection between the unstable periodic orbit and the region where the numerically observed attractor exists. Hence we cannot state for sure that the unstable fixed point P_3 does not belong to the attractor.

The nonwandering region contains all periodic orbits and ω–limit sets for the system. Hence in the search for periodic orbits we may limit ourselves to the region

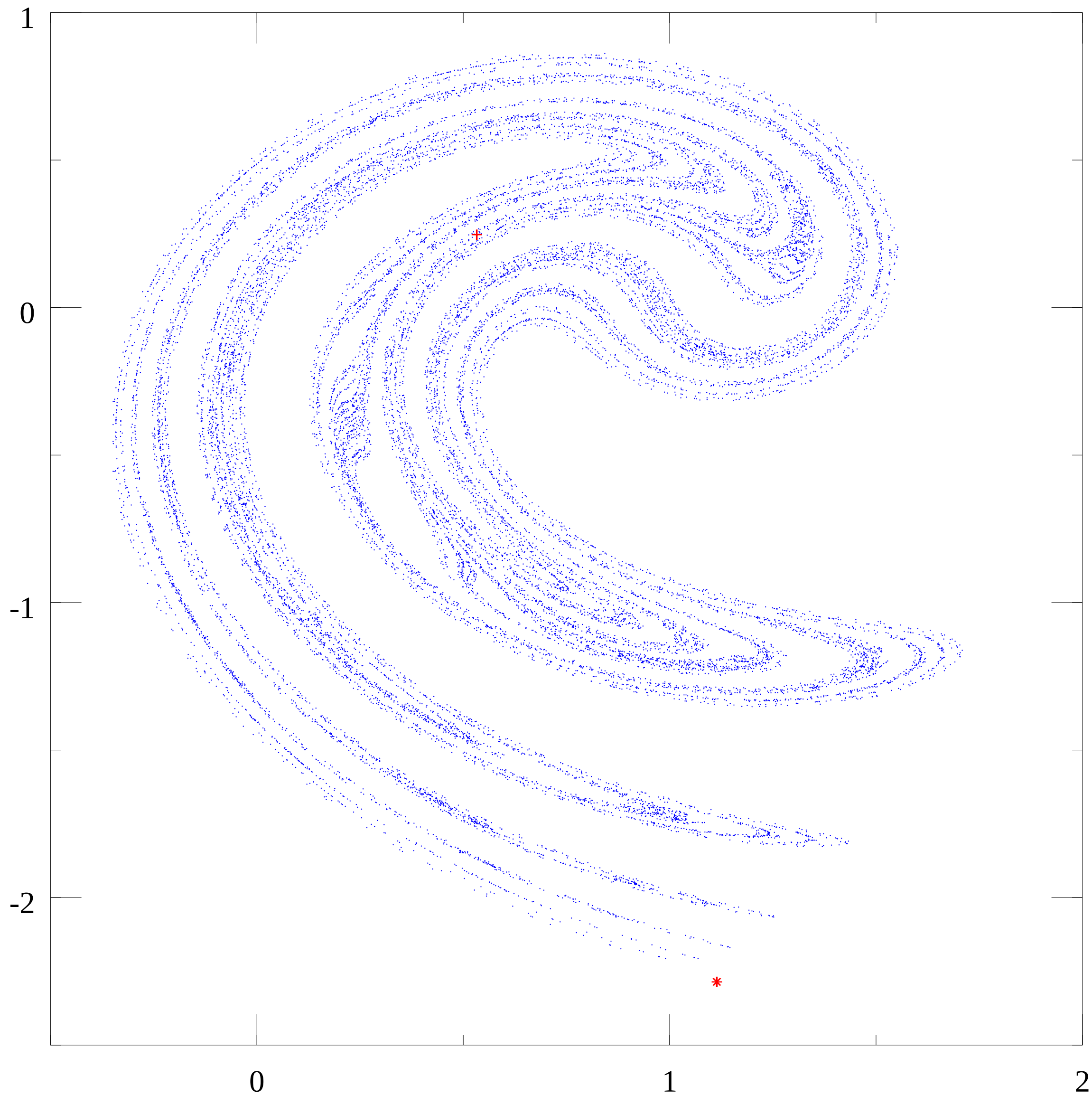

Figure 9: Ikeda map, a chaotic trajectory, the unstable point inside the attractor (+) and unstable fixed point located slightly below the attractor ($*$).

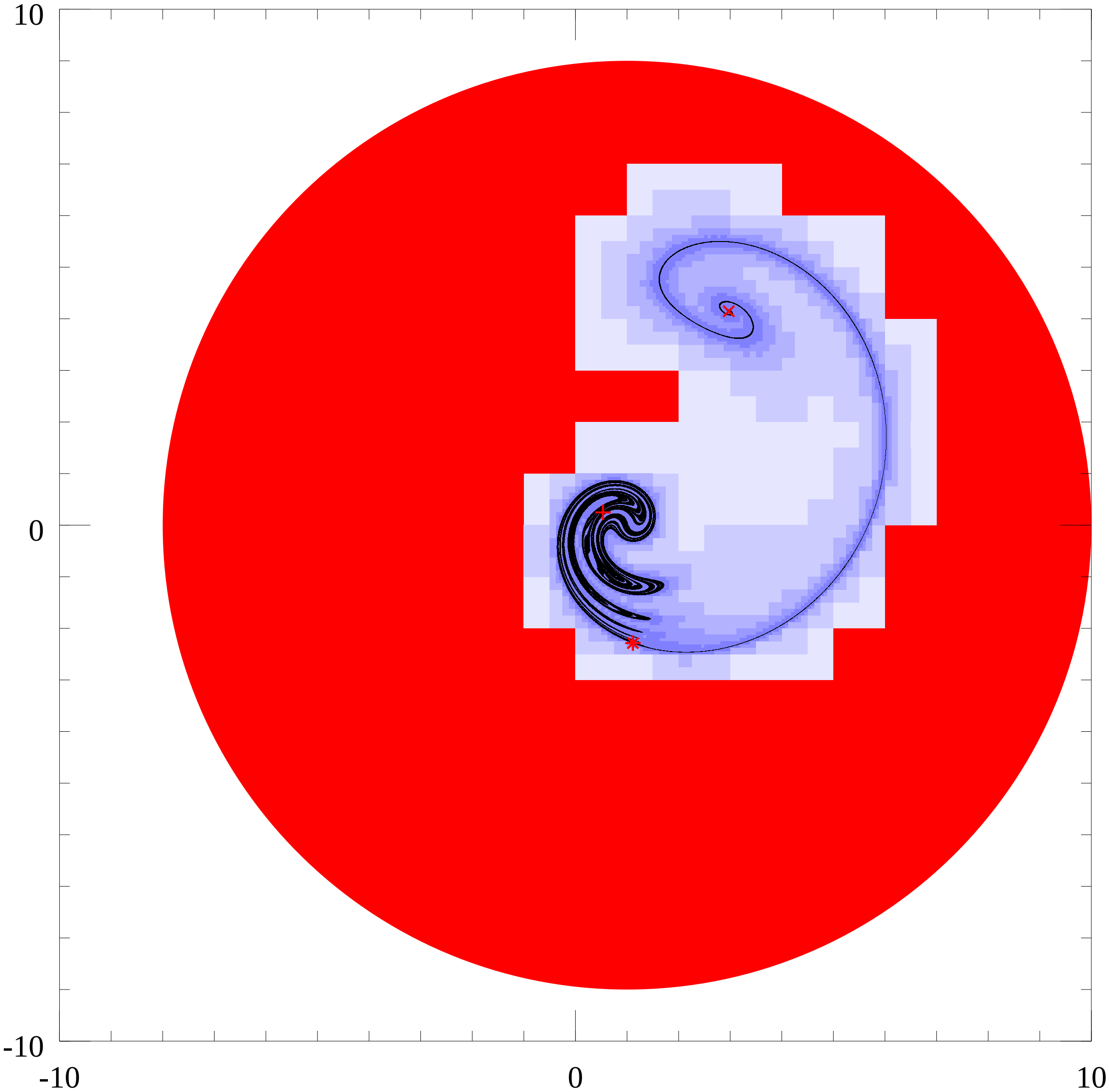

Figure 10: Ikeda map, invariant part of the trapping, the stable fixed point P_1 ($\times$) and the unstable fixed points P_2 and P_3 ($+$,$\ast$).

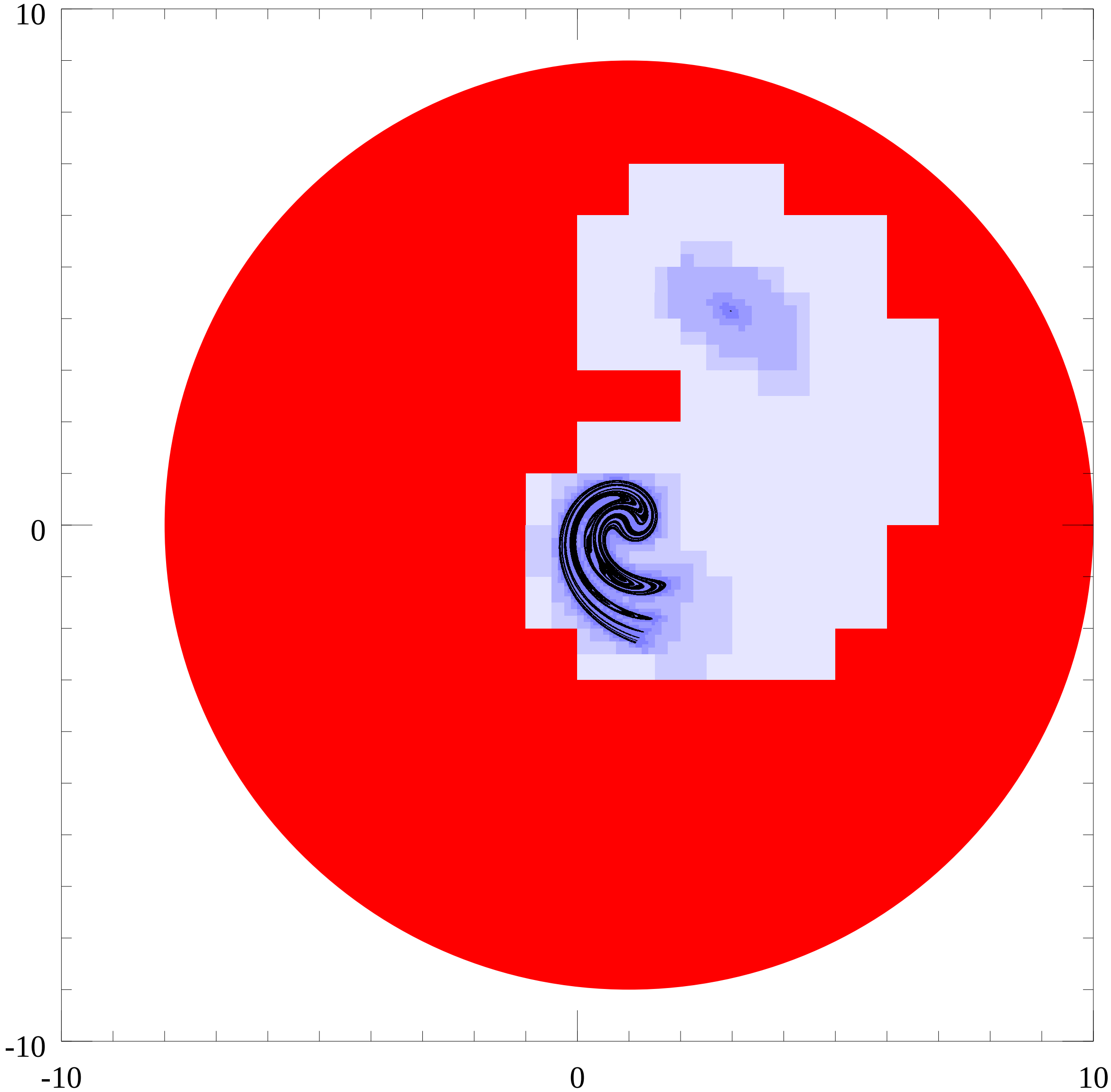

Figure 11: Ikeda map, nonwandering part of the trapping region.

containing the nonwandering part, area of which is much smaller than the area of the trapping region 254.5.

In order to better understand the dynamics of the system we have found the basin of attraction of the stable fixed point P_1. First, we have located a trapping region around the stable fixed point. The size and the shape of the basin of attraction is a global feature and cannot be studied by means of the Jacobian matrix at the stable fixed point alone. However, analysis of the Jacobian matrix helps us to choose the initial trapping region. Close to the fixed point when the linear approximation is valid, we may easily find a small set, which is a trapping region. For the algorithm `FindBasin` this set should be as large as possible. The matrix norm induced by the Euclidean norm for the Jacobian matrix at P_1 is $1.753 > 1$. This means that in the linear approximation circles are not trapping regions and we need to start with an ellipse. We have found that the following ellipse is a trapping region for the map:

$$\begin{aligned}&\left(\frac{\cos^2\varphi}{r_1^2}+\frac{\sin^2\varphi}{r_2^2}\right)(x-x_0)^2+\left(\frac{\sin^2\varphi}{r_1^2}+\frac{\cos^2\varphi}{r_2^2}\right)(y-y_0)^2+\\&\left(\frac{1}{r_1^2}-\frac{1}{r_2^2}\right)\sin(2\varphi)(x-x_0)(y-y_0)\leq 1,\end{aligned} \tag{21}$$

where $x_0 = 2.972132$, $y_0 = 4.145946$, $r_1 = 1.2$, $r_2 = 2.1$, $\varphi = 1$. Then using the hyperbolicity of the fixed point we have shown that the invariant part of this trapping region is P_1 (all trajectories starting in the ellipse converge to the fixed point).

Finally using the algorithm `FindBasin` we have found a subset of the rectangle $[-10, 10] \times [-10, 10]$ enclosed in the basin of attraction of P_1 (see Fig. 12). The region found has an area of 357.005. Since in each basin of attraction there is only one periodic orbit once we locate this orbit we may exclude the basin of attraction from the region where we search for other periodic orbits.

5.1 Periodic orbits with period $n \leq 15$

We have found all periodic orbits for the Ikeda map with period smaller or equal to 15. For the standard version, the Krawczyk and Hansen–Sengupta operators are 2 or 3 times faster than the Newton operator is. However for the global version there are no significant differences in computation time. The results are collected in Table 5. Periodic orbits found are shown in Fig. 13 and 14. One can see that low–period cycles do not fill the attractor uniformly and an interesting Cantor set like structure is formed. As for the Hénon map we compute the closest neighbor distance and summarize the results in Table 6.

5.2 Estimation of topological entropy

As before we use the formula (18) to estimate the topological entropy of the map. The values of $\mathrm{H}_n(h) = \log(\mathrm{P}_n)/n$ for different n are collected in Table 5 and plotted in Fig. 15. The approximation stabilizes as n is increased. This lets us state the hypothesis that the topological entropy of the Ikeda map for the parameters considered is $\mathrm{H}(f) \approx 0.6$.

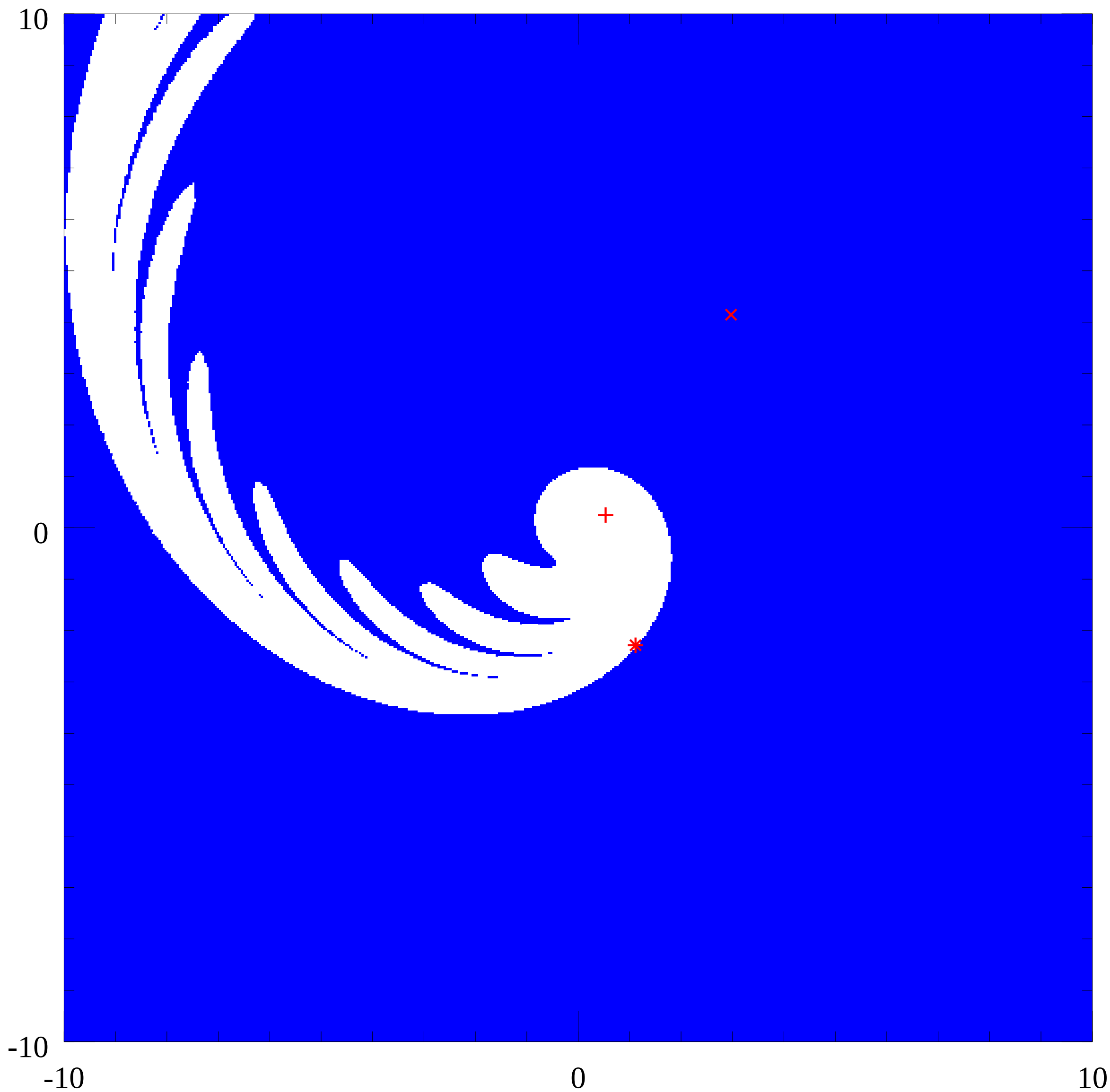

Figure 12: Ikeda map, basin of attraction of the stable fixed point P_1 ($\times$), the unstable fixed point P_2 ($+$) belonging to the attractor and the unstable fixed point P_3 ($\ast$) lying on the border of the basin of attraction of P_1.

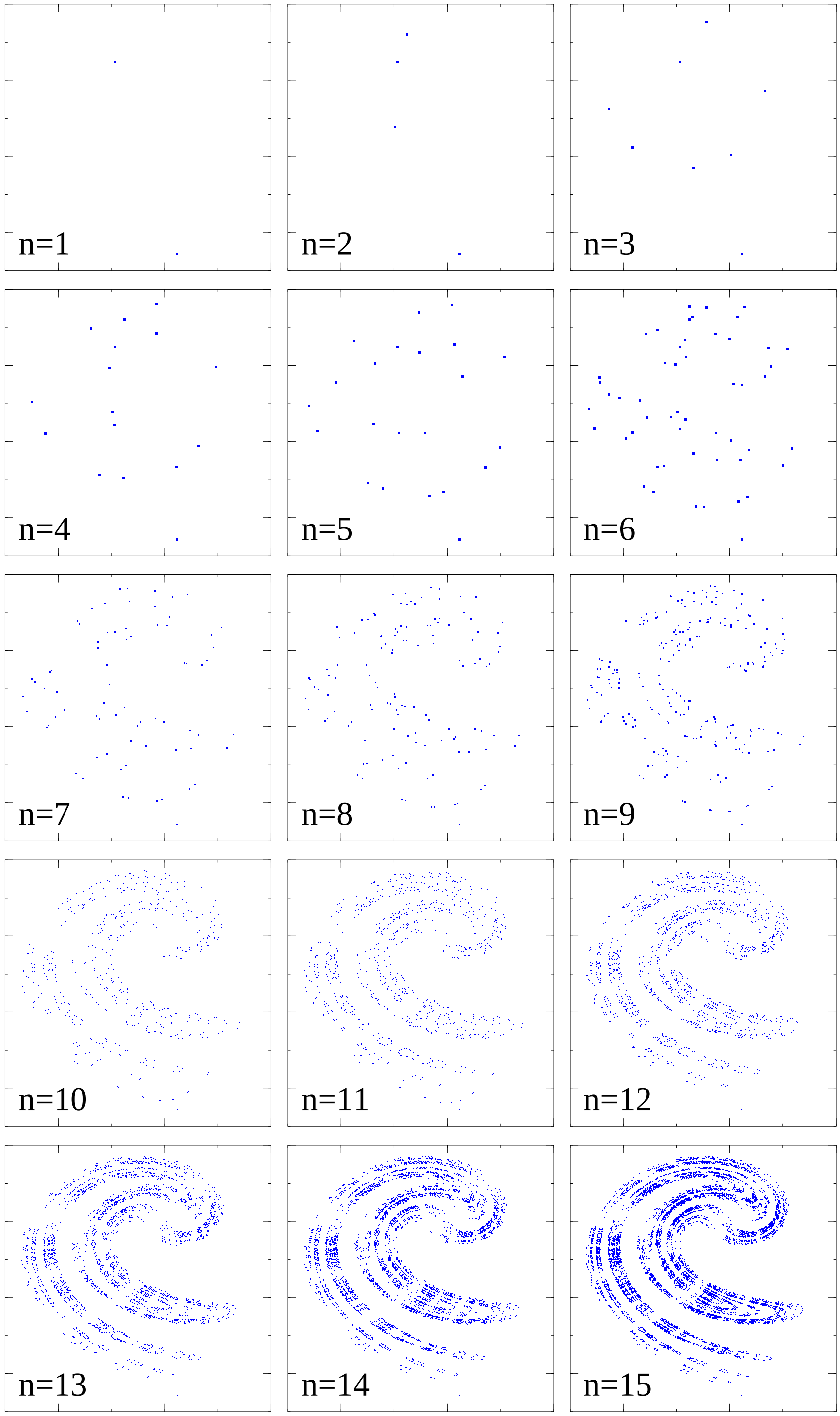

Figure 13: Ikeda map, periodic orbit with period $n \leq 15$.

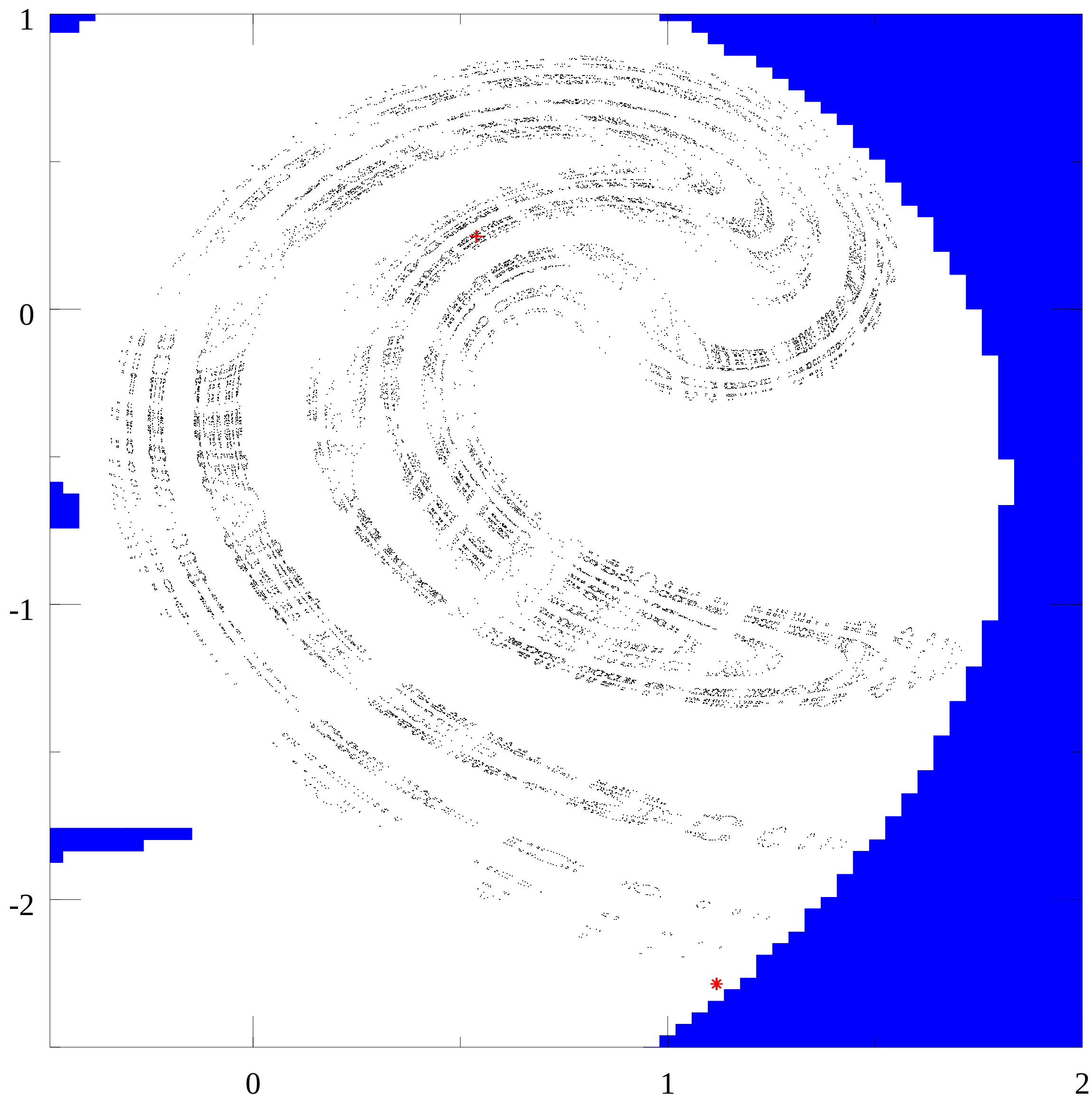

Figure 14: Ikeda map, periodic orbits with period $n = 1, \ldots, 15$, basin of attraction of P_1

n	Q_n	P_n	$Q_{\leq n}$	$P_{\leq n}$	H_n
1	2	2	2	2	0.6931
2	1	4	3	4	0.6931
3	2	8	5	10	0.6931
4	3	16	8	22	0.6931
5	4	22	12	42	0.6182
6	7	52	19	84	0.6585
7	10	72	29	154	0.6110
8	14	128	43	266	0.6065
9	26	242	69	500	0.6099
10	46	484	115	960	0.6182
11	76	838	191	1796	0.6119
12	110	1384	301	3116	0.6027
13	194	2524	495	5638	0.6026
14	317	4512	812	10076	0.6010
15	566	8518	1378	18566	0.6033

Table 5: Q_n — number of periodic orbits with period n, P_n — number of fixed points of f^n, $Q_{\leq n}$ — number of cycles with period smaller or equal to n, $P_{\leq n}$ — number of fixed points of f^i for $i \leq n$, $H_n = n^{-1}\log(P_n)$ — estimation of topological entropy.

n	P_n	D_c	D_e	$D_{\min}$	$D_{\max}$	D_{av}
1	2	$3.19 \cdot 10^{-2}$	$2.98 \cdot 10^{-14}$	2.599	2.599	2.599
2	4	$1.69 \cdot 10^{-3}$	$2.98 \cdot 10^{-14}$	0.370	1.783	0.8445
3	8	$6.37 \cdot 10^{-4}$	$3.38 \cdot 10^{-14}$	0.395	1.220	0.6442
4	16	$8.01 \cdot 10^{-5}$	$3.56 \cdot 10^{-14}$	0.175	0.956	0.3739
5	22	$8.01 \cdot 10^{-5}$	$3.85 \cdot 10^{-14}$	0.143	0.644	0.3033
6	52	$2.40 \cdot 10^{-5}$	$5.20 \cdot 10^{-14}$	$4.27 \cdot 10^{-2}$	0.495	0.1404
7	72	$3.48 \cdot 10^{-6}$	$6.89 \cdot 10^{-14}$	$1.98 \cdot 10^{-2}$	0.355	0.1057
8	128	$1.23 \cdot 10^{-6}$	$1.41 \cdot 10^{-13}$	$4.56 \cdot 10^{-2}$	0.264	0.0726
9	242	$7.80 \cdot 10^{-8}$	$5.89 \cdot 10^{-13}$	$7.39 \cdot 10^{-4}$	0.210	0.0456
10	484	$5.92 \cdot 10^{-8}$	$2.72 \cdot 10^{-13}$	$1.25 \cdot 10^{-3}$	0.143	0.0310
11	838	$1.26 \cdot 10^{-8}$	$3.25 \cdot 10^{-13}$	$7.22 \cdot 10^{-4}$	0.119	0.0226
12	1384	$5.25 \cdot 10^{-9}$	$2.92 \cdot 10^{-13}$	$4.11 \cdot 10^{-4}$	0.337	0.0160
13	2524	$2.06 \cdot 10^{-9}$	$3.12 \cdot 10^{-13}$	$2.55 \cdot 10^{-4}$	0.270	0.0109
14	4512	$4.13 \cdot 10^{-10}$	$8.36 \cdot 10^{-13}$	$7.01 \cdot 10^{-5}$	0.260	0.00753
15	8518	$8.08 \cdot 10^{-11}$	$5.14 \cdot 10^{-13}$	$1.02 \cdot 10^{-4}$	0.197	0.00515

Table 6: P_n — number of fixed points of f^n, D_c — diameter of interval for which uniqueness was proved, D_e — diameter of interval for which existence was proved, closest neighbor distance: minimum $D_{\min}$, maximum $D_{\max}$, average D_{av}.

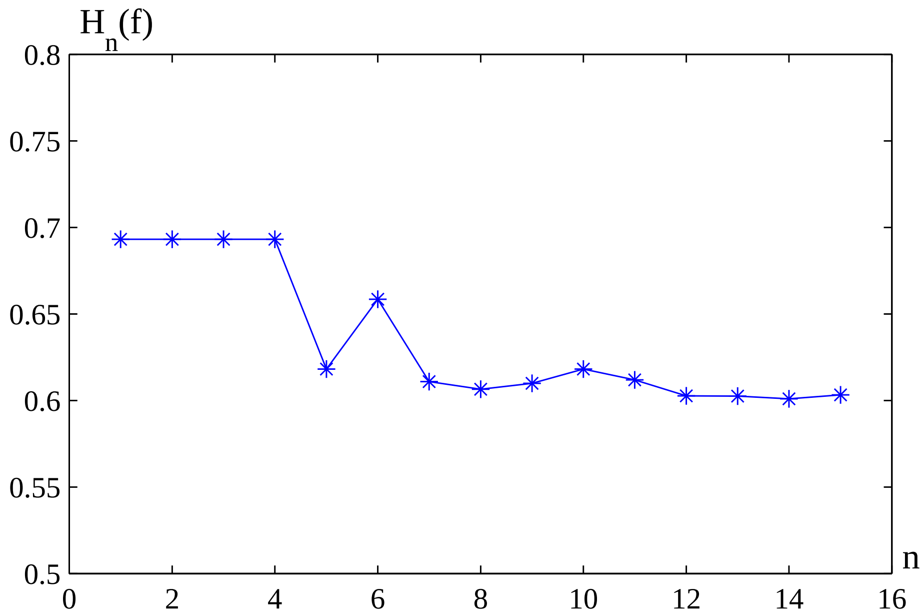

Figure 15: Estimation of topological entropy for the Ikeda map based on the number of short periodic orbits.

6 Conclusions

In this paper we have shown that interval arithmetic is a very powerful tool for investigations of nonlinear systems and rigorous studies of periodic orbits in particular. We have described methods for computation of the enclosure of the invariant part and the nonwandering part of a given set. We have also developed methods for finding all low period cycles for the discrete–time dynamical systems based on interval operators. We have compared the performance of several interval methods. We have shown that the global version with the reduced search space is superior to all other methods. We have also shown that for the maps considered using Krawczyk or Hansen–Sengupta operators does not reduce the computational time considerably. It is true however that there exist systems for which Newton operator is significantly slower then the two other operators. A very simple example is the non–invertible logistic map.

Using these methods we have found all periodic orbits for the Hénon map with period $n \leq 30$ and for the Ikeda map with period $n \leq 15$ and estimated the topological entropy of these maps.

It was shown that the information about periodic orbits which can be obtained using the presented methods allows to investigate further the structure of chaotic attractors. First, the number of periodic orbits gives us a good approximation of invariants like topological entropy. The convergence of the approximation is considerably fast. Second, we can easily identify regions within the chaotic attractor not visited by short cycles and this gives us better insight into the structure of the attractor.

The methods presented can also be applied to investigate periodic orbits for continuous–time systems by using the technique of Poincaré map [Galias, 1999].

Acknowledgments

This paper has been prepared in part during the author's stay at the Institute for Nonlinear Science, University of California, San Diego, USA, sponsored by the Fulbright fellowship. This work was supported in part by ARO, grant No. DAAG 55–98–1–0269.

Appendix

In the appendix we present a simple proof of the theorem on the existence, uniqueness, and nonexistence of zeros of a map using interval Newton operator.

Theorem 2. *Let $f : \mathbb{R}^n \supset D \mapsto \mathbb{R}^n$ be a continuously differentiable mapping. Let $\mathbf{x} \subset D$ be an interval vector and let us choose $x_0 \in \mathbf{x}$. $f'(\mathbf{x})$ is the interval arithmetic evaluation of the Jacobian of f over the interval $\mathbf{x}$. We assume that $f'(\mathbf{x})^{-1}$ exists. Let $\mathbf{N}(\mathbf{x}) = x_0 - f'(\mathbf{x})^{-1} f(x_0)$.*

(i). *If $\mathbf{N}(\mathbf{x}) \cap \mathbf{x} = \emptyset$ then f has no zero in $\mathbf{x}$.*

(ii). *If $\mathbf{N}(\mathbf{x}) \subset \mathbf{x}$ then f has a unique zero in $\mathbf{x}$.*

Proof. Let $g(t) = f(x_0 + t(x - x_0))$. It is clear that

$$f(x) - f(x_0) = g(1) - g(0) = \int_0^1 g'(t)dt = \int_0^1 f'(x_0 + t(x - x_0))(x - x_0)dt, \qquad (22)$$

Hence

$$f(x) - f(x_0) = J(x)(x - x_0), \qquad (23)$$

where

$$J(x) = \int_0^1 f'(x_0 + t(x - x_0))dt. \qquad (24)$$

If $x, x_0 \in \mathbf{x}$ and $t \in [0,1]$ then $x_0 + t(x - x_0) \in \mathbf{x}$ as the interval vector $\mathbf{x}$ is convex. Hence $J(x) \in f'(\mathbf{x})$. From the existence of $f'(\mathbf{x})^{-1}$ it follows that $f'(\mathbf{x})$ does not contain any singular matrix and hence $J(x)$ is nonsingular for all $x \in \mathbf{x}$.

(i). First we show that if f has a zero $x^\star$ in $\mathbf{x}$ then $x^\star \in \mathbf{N}(\mathbf{x})$. The first part of the theorem will then follow.

$$J(x^\star)(x^\star - x_0) = f(x^\star) - f(x_0) = -f(x_0). \qquad (25)$$

Since $J(x^\star) \in f'(\mathbf{x})$ it is nonsingular and therefore $x^\star = x_0 - J(x^\star)^{-1} f(y) \in x_0 - f'(\mathbf{x}) f(x_0) = \mathbf{N}(\mathbf{x})$. It is clear that if $\mathbf{x} \cap \mathbf{N}(\mathbf{x}) = \emptyset$ then $\mathbf{x}$ contains no zeros of f.

(ii). Let us define $p(x) = x_0 - J(x)^{-1}f(x_0)$.

$$p(x) = x_0 - J(x)^{-1}f(x_0) \in \mathbf{N}(\mathbf{x}) \subset \mathbf{x}. \tag{26}$$

for all $x \in \mathbf{x}$. Since $p(\mathbf{x}) \subset \mathbf{x}$ by Brouwer's fixed point theorem there exists $x^\star$ such that $p(x^\star) = x^\star$. Then

$$\begin{aligned} 0 &= p(x^\star) - x^\star = x_0 - J(x^\star)^{-1}f(x_0) - x^\star \\ &= x_0 - J(x^\star)^{-1}(f(x^\star) - J(x^\star)(x^\star - x_0)) - x^\star \\ &= x_0 - J(x^\star)^{-1}f(x^\star) + x^\star - x_0 - x^\star = -J(x^\star)^{-1}f(x^\star). \end{aligned}$$

Since $J(x^\star)$ is nonsingular $f(x^\star) = 0$.

Now we prove the uniqueness of the fixed point. Assume that $x^\star$ and $x^{\star\star}$ are two zeros of f in $\mathbf{x}$. We will show that from the existence of $f'(\mathbf{x})^{-1}$ if follows that they must be equal.

$$J(x^\star)(x^\star - x^{\star\star}) = f(x^\star) - f(x^{\star\star}) = 0, \tag{27}$$

where

$$J(x^\star) = \int_0^1 f(x^{\star\star} + t(x^\star - x^{\star\star}))dt. \tag{28}$$

As $J(x^\star)$ is nonsingular it follows that $x^\star = x^{\star\star}$.

$\square$

References

Alefeld, G. [1994] Inclusion Methods for Systems of Nonlinear Equations – The Interval Newton Method and Modifications, *in* J. Herzberger, ed., "Topics in Validated Computations", IMACS–GAMM, pp. 7–26.

Alefeld, G. & Herzberger, J. [1983] *Introduction to interval computations*, Academic Press, New York.

Bowen, R. [1971] "Periodic points and measures for axiom A diffeomorphisms", *Trans. Amer. Math. Soc.* **154**, 377–397.

Galias, Z. [1998*a*] Existence and uniqueness of low–period cycles and estimation of topological entropy for the Hénon map, *Proc. Int. Symposium on Nonlinear Theory and its Applications, NOLTA'98*, Vol. 1, Crans–Montana, pp. 187–190.

Galias, Z. [1998*b*] "Rigorous numerical studies of the existence of periodic orbits for the Hénon map", *J. of Universal Computer Science, Springer* **4**(2), 114–124. (http://www.iicm.edu/jucs_4_2).

Galias, Z. [1999] Rigorous investigations of periodic orbits in an electronic circuit by means of interval methods, *Proc. Int. Workshop, Nonlinear Dynamics of Electronics Systems, NDES'99*, Rønne, pp. 41–44.

Galias, Z., Nossek, J. & Ogorzałek, M. [1994] Negative results on control of chaotic circuits, *Proc. Int. Workshop, Nonlinear Dynamics of Electronics Systems, NDES'94*, Cracow, pp. 174–178.

Gibbons, A. [1985] *Algorithmic graph theory*, Cambridge University Press, Cambridge.

Hammel, S., Jones, C. & Moloney, J. [1985] "Global dynamical behavior of the optical field in a ring cavity", *J. Opt. Soc. Am. B* **2**(4), 552–564.

Hayes, S. & Grebogi, C. [1995] Using chaos for digital communication, *in* T. Carroll & L. Pecora, eds, "Nonlinear Dynamics in Circuits", World Scientific, pp. 325–335.

Hénon, M. [1976] "A two dimensional map with a strange attractor", *Commun. Math. Phys.* **50**, 69–77.

Kearfott, R. & Novoa, M. [1990] "Algorithm 681: INTBIS, a portable interval Newton/bisection package", *ACM Trans. Math. Software* **16**(2), 152–157.

Krasnosielskij, M. [1963] *Wektornyje pola na ploskosti*, FM, Moscow. in russian.

Lathrop, D. & Kostelich, E. [1989] "Characterisation of an experimental strange attractor by periodic orbits", *Phys. Rev. A* **40**(7), 4028–4031.

Miranda, C. [1940] "Un'osservazione su un teorema di Brouwer", *Boll. Un. Mat. Ital.* **2**(3), 5–7.

Moore, R. [1979] *Methods and applications of interval analysis*, SIAM, Philadelphia.

Neumaier, A. [1990] *Interval methods for systems of equations*, Cambrigde University Press.

Ott, E., Grebogi, C. & Yorke, J. [1990] Controlling chaotic dynamical systems, *in* D. Campbell, ed., "Chaos — Soviet-American Perspectives on Nonlinear Science", American Institute of Physics, New York, pp. 153–172.

Zgliczyński, P. [1997] "Computer assisted proof of chaos in the Rössler equations and the Hénon map", *Nonlinearity* **10**(1), 243–252.